ARL-FLIGHT-MECH-R-179

AR-005-607

AD-A236 026

AUSTRALIA

DEPARTMENT OF DEFENCE

DEFENCE SCIENCE AND TECHNOLOGY ORGANISATION

AERONAUTICAL RESEARCH LABORATORY

MELBOURNE, VICTORIA

Flight Mechanics Report 179

WATER TUNNEL FLOW VISUALISATION OF VORTEX BREAKDOWN OVER THE F/A-18

by

D.H. THOMPSON

Approved for public release

91-01071

DECEMBER 1990

AR-005-607

DEPARTMENT OF DEFENCE
DEFENCE SCIENCE AND TECHNOLOGY ORGANISATION
AERONAUTICAL RESEARCH LABORATORY

Flight Mechanics Report 179

WATER TUNNEL FLOW VISUALISATION OF VORTEX BREAKDOWN OVER THE F/A-18

by

D.H. THOMPSON

A-1

SUMMARY

Vortex flow patterns over models of the F/A-18 aircraft were visualised using dye and hydrogen bubble techniques in a water tunnel. The axial position of vortex breakdown in the leading-edge extension (LEX) vortices was measured, and was found to be insensitive to Reynolds number, to flap setting, and to small variations in model cross-section shape. Engine inlet flow did alter the vortex breakdown position, at flow rates that might be encountered under flight conditions. The fitting of fences on the LEX upper surface did not affect the axial position of vortex breakdown, but did alter the vortex structure. These alterations were examined in some detail.

DSTO ARL MELBOURNE

POSTAL ADDRESS: Director, Aeronautical Research Laboratory
506 Lorimer Street, Fishermens Bend Victoria 3207
Australia

CONTENTS

NOTATION

LEX	Leading Edge eXtension
R_{mac}	Reynolds number based on mean aerodynamic chord
LEF	Leading Edge Flap
TEF	Trailing Edge Flap
X	Distance from aircraft nose, measured along longitudinal axis of aircraft
L	Length of aircraft, from fuselage nose to exhaust nozzle exit plane
V_I	Mean velocity at engine inlet plane
V_0	Freestream velocity

1. INTRODUCTION

The flow around the F/A-18 aircraft at moderate to high angles of attack is complex and is dominated by the separated vortices generated by the highly-swept wing leading-edge root extensions (LEXes). The vortices pass over the rear fuselage of the aircraft, and the vertical and horizontal tail surfaces are immersed in the vortical flow field.

The pressure field due to the vortices contributes substantially to the generation of lift on the aircraft, allowing routine flight manoeuvres at angles of attack of 35^{o} or more. However, the phenomenon of vortex breakdown can lead to adverse effects on the aircraft structure. Vortex breakdown occurs when the stable core of a LEX vortex undergoes a sudden expansion. Flow reversal in the core occurs, and the flow downstream of the breakdown point becomes disturbed and unsteady. The impingement of the unsteady flow on the tail surfaces leads to structural vibration, particularly of the vertical fins.

The flow around the F/A-18 has been studied in some detail in water tunnel tests by Erickson[1], and in wind tunnel tests by Erickson et al [2]. Water and wind tunnel test results have been reported by Lee et al[3], and by Wentz[4]. In the study described in this report, the flow around a model of the F/A-18 was visualised in a water tunnel. The effects of aircraft geometry and engine inlet flow on vortex breakdown position were measured for a range of angles of attack and flow velocity. Also, the effects of modifications developed by the aircraft's manufacturer to reduce the structural impact of vortex breakdown were studied.

2. EXPERIMENTAL PROCEDURE

2.1 Test facilities

Most of the tests described here were carried out in the ARL Flight Mechanics Branch water tunnel (Fig.1). This is an Eidetics Model 1520 horizontal-flow tunnel, with a test section 380 mm wide, 510 mm deep, and 1.52 m long. The tunnel is operated with a free surface in the test section. The model is mounted inverted in the test section, on a support system consisting of a sting and C-strut, and is positioned in pitch and yaw by remotely-controlled DC motors. Readouts of pitch and yaw angle are provided on the tunnel control panel.

Also included in this report are some earlier results of F/A-18 vortex breakdown measurements made in a smaller vertical water tunnel (250 mm x 250 mm test section) and in a small towing tank (300 mm x 300 mm cross-section).

2.2 Models

The model used in the majority of the tests described here was a 1/48 scale model of the F/A-18 (Fig.2). A standard plastic hobby kit (Monogram brand) was modified to make it suitable for test purposes. The model outline was checked carefully against drawings and photographs of the full-scale aircraft, and some changes were made to the model to improve its accuracy. Dye ports were positioned at various points on the surface of the model. The connecting tubes from these ports were led internally to the rear of the fuselage where they were brought out of the model to pass back along the sting to the model support system. To provide access to the tubes within the model, a section of the upper fuselage, including the cockpit canopy, was made removable.

By inserting tranverse bulkheads and longitudinal partitions inside the model, two closed ducts were formed, one leading from each engine inlet to the corresponding exhaust nozzle. A length of brass tube was cemented into each nozzle, extending behind the aircraft. Each tube could be connected to a suction pump through an individual flow meter. This arrangement allowed independent control of the flow into each inlet. In addition, the exhaust tubes, clamped in a suitable fitting, served to mount the model on the sting of the model support system.

The wing leading-edge and trailing-edge flaps were cut away from the wing structure, and could be re-attached at various deflection settings by means of simple bent-metal brackets attached to the wing and flap undersurfaces with double-sided adhesive tape. Each horizontal tail surface was mounted on a spanwise spindle, and could be locked at any desired deflection angle by means of a small set-screw in the fuselage.

The model could be fitted with LEX fences. These are streamwise trapezoidal plates fixed normal to the LEX upper surface, at about the LEX semi-span, just ahead of the LEX/wing leading-edge junction (Fig.3). The fences were developed by the manufacturer of the F/A-18, and their purpose is to modify the vortex/fin interaction to reduce the unsteady structural loading on the fin. The fences are being fitted to all new production F/A-18 aircraft, and retrofitted to older aircraft.

Another 1/48 scale F/A-18 model was used to provide some comparative results in the test program. This model, also assembled from a plastic hobby kit (Revell brand), was supplied by the water tunnel manufacturer as a demonstration model. It incorporated dye ports and an engine inlet flow system, but had no provision for variable flap or horizontal tail settings.

The earlier vertical water tunnel and towing tank results mentioned above were obtained using a 1/72 scale model. This also was assembled from a hobby kit, but had no dye ports or engine inlet flow provisions. Both the flap and horizontal tailplane settings were adjustable.

Two techniques were used for flow visualisation. The first of these involved the injection of coloured dyes through ports in the model surface. Several dye ports were positioned around the model nose, and on the fuselage sides ahead of the engine inlets. One port was positioned just beneath each LEX apex, one on each LEX upper surface, and one on each LEX lower surface. Liquid food dyes were used for most of the tests, with the occasional use of fluorescein sodium, a fluorescent dye.

The dyes were supplied from containers pressurised by air from a small compressor. The dye flow rate was controlled by a needle valve in each dye line, and up to six independently controlled dye lines were available at any one time. The six lines passed through a channel in the C-strut of the model support system, and were connected to selected tubes emerging from the rear of the model.

Flow patterns were also visualised using the hydrogen bubble technique, which involved the electrolytic generation of minute hydrogen gas bubbles to act as flow tracers. This technique is particularly suited to the visualisation of the separated vortex flows above highly-swept surfaces like the F/A-18 LEX. The cathode of the electrolytic circuit consisted of a narrow strip of aluminium foil cemented beneath the leading-edge of the LEX. The anode was another foil strip cemented to the LEX undersurface, close to the fuselage side. Bubbles from the cathode strip were swept from the leading-edge into the vortex system above the LEX.

General illumination of the model and dye patterns was provided by a 1000 W quartz-iodine lamp mounted beneath the test section, together with 3 x 150 W tungsten spotlamps mounted in front of the test section. For the hydrogen bubbles, illumination was provided by 2 x 150 W tungsten spotlamps mounted beneath the test section.

Considerable insight into the structure of the vortical flows can be gained by illuminating the flow patterns in a cross-flow plane, using a laser light sheet. This approach is particularly effective when used with hydrogen bubbles shed from the LEX leading-edge. The laser light sheet was generated using a Lexel Model 65 air-cooled argon ion laser, producing about 35 mW of power at a wavelength of 488 nm. The laser was set up beneath the test section. The output beam was expanded into a fan by means of a glass rod, and reflected up into the test section by a small scanning mirror. The scanning mirror could be driven to preselected angles to place the light sheet at different positions on the model. Alternatively, the mirror could be driven by a triangular or sawtooth wave form to sweep the light sheet repeatedly through the flow volume of interest.

The configuration of the Eidetics water tunnel is designed specifically to allow convenient viewing of cross-flow planes via the window at the end of the discharge section, downstream of the test section. Thus it is not necessary to insert a mirror into the flow behind the model to obtain the desired viewing angle.

Earlier results with the 1/72 scale F/A-18 model were obtained using dye in the vertical water tunnel and hydrogen bubbles in the towing tank. As this model had no surface dye ports, dye was injected through a probe upstream of the model. The probe position was adjusted until the injected dye filament passed around the model nose and into the LEX vortex core.

2.4 Recording of results

Extensive use was made of video techniques in recording the results of these flow visualisation tests. For general recording of dye patterns, two monochrome CCD video cameras were used. One was mounted in front of the test section to provide side views of the model. The other was mounted beneath the test section and provided plan views. To record cross-flow plane views, a third camera, of the same type, was positioned at the downstream viewing window, looking upstream into the test section.

The cameras were used in conjunction with a PC-based image acquisition and processing system. A program written using Imaging Technology ITEX PCplus library routines allowed two images, one from each of two video cameras, to be grabbed in succession and stored in the image processor board's memory. In these tests, the two images were respectively a plan view and a side view of the model and flow pattern. Subsequently, each image could be titled and stored on disk if required. Model angle of attack and the position of flow features such as vortex breakdown could be measured directly from the video images by means of a cursor. Scaling was accomplished by including a grid in the field of view of the video camera, and by placing reference marks on the model. Calculation and plotting of the vortex breakdown position were performed by appropriate programs on the PC. Finally, a hard-copy print of any image could be produced if required using a Mitsubishi P75E Video Copy Processor. A typical print from this machine is shown in Fig.4.

Cross-flow plane images also could be acquired using the same system. In addition, most flow patterns were recorded on videotape. Conventional film photography was used to provide higher quality images of selected flow patterns.

2.5 Test program

To establish a reference set of measurements, vortex breakdown axial positions were measured for a leading-edge flap / trailing-edge flap (LEF/TEF) setting of $35^{0}/0^{0}$, at a flow velocity of 80 mm/s. Further tests were carried out at this flap setting over a range of flow velocities from 40 mm/s to 360 mm/s. Additional flap setting combinations of $35^{0}/35^{0}$, $0^{0}/0^{0}$, and $0^{0}/35^{0}$ were tested at a flow velocity of 80 mm/s. The effects of airbrake and horizontal stabilator deflection were also examined. The effects of engine inlet flow were evaluated for two leading-edge flap settings and a range of inlet flow velocities.

Vortex breakdown positions were measured for the model fitted with the LEX fences. Additional tests were carried out to determine in more detail the effects of the LEX fence on the flow above the LEX and wing, in an attempt to explain how the fences produce their apparently favourable effect on the vertical fin unsteady flow environment.

3. RESULTS AND DISCUSSION

3.1 Reference configuration

Fig.5 shows plan and side views of the F/A-18 model over a range of angles of attack in the water tunnel test section. The model is in the reference configuration, and the core of each LEX vortex is marked by dye injected through the port located beneath the apex of each LEX. Stretching downstream from the LEX apex, the core dye filament remains slender and compact until a point is reached where it expands suddenly. The sudden expansion marks the occurrence of vortex breakdown, and downstream of the breakdown, the flow in the core is unsteady. The vertical fin is immersed in this unsteady flow. (It should be noted that the apparent double breakdown visible in some of the plan view photographs is due to the shadow of the breakdown falling on the upper surface of the model.)

The vortex breakdown moves upstream as the angle of attack is increased. Fig.5(a) shows that at an angle of attack of 19.5°, breakdown occurs just ahead of and just outboard of the fin leading-edge. At an angle of attack of 25.4°, (Fig.5(b)), the breakdown has moved upstream to a point just aft of the junction between the wing and LEX leading-edges. The upstream movement continues until, at an angle of attack of 40.3°, the breakdown is in the vicinity of the cockpit.

The variation of vortex breakdown axial position with angle of attack, for a flap setting of $35^{\circ}/0^{\circ}$ and a flow velocity of 80 mm/s, is shown in Fig.6. The Reynolds number based on mean aerodynamic chord (R_{mac}) was 5120. The engine inlet suction system was not connected, the inlets being in a flow-through configuration.

At any particular test point, the vortex breakdown position usually was not steady, but moved irregularly upstream and downstream over a short distance. Also, there was sometimes some asymmetry between the port and starboard vortex breakdown positions. For these reasons, there is some scatter in the results - typically, about 5 - 10% of the model length. This seems to be typical of other experimental measurements of vortex breakdown position over aircraft configurations reported in the literature.

3.2 Effect of Reynolds number

Fig.7 shows the effects of variations in tunnel flow velocity on vortex breakdown position. Tests were performed at velocities of 42, 74, 120 and 366 mm/s, corresponding respectively to R_{mac} values of 2688, 4736, 7680, and 23424, in addition to the reference case of 80 mm/s. Fig.6 shows that any variations due to flow velocity fall within the scatter of the measured breakdown positions, for a Reynolds number variation of about one order of magnitude.

In Fig.8, the water tunnel results are compared to wind tunnel and flight results taken from Ref.2. The wind tunnel results were obtained at $R_{mac} = 1.75 \times 10^6$, and the flight results at $R_{mac} = 1.35 \times 10^7$. Also included are some unpublished results of measurements made on a 1/9 scale model in the ARL Flight Mechanics Branch low-speed wind tunnel ($R_{mac} = 1.34 \times 10^5$). The agreement between results covering almost four orders of magnitude in Reynolds number is remarkably close. There appears to be a slight upstream shift of the breakdown position with increasing Reynolds number at a given angle of attack, but the magnitude of this shift is little greater than the overall scatter of the results. This relative independence of breakdown position on Reynolds number justifies investigations of the phenomenon using small-scale models in water tunnels at low speeds.

3.3 Effect of flap settings

At moderate to high angles of attack, the flow over the outer wing panels of the F/A-18 is strongly influenced by the deflection of the flaps, particularly the leading-edge flaps. It was thought that changes in outer wing flow due to flap deflection might influence the location of vortex breakdown. In addition, the downward deflection of the leading-edge flap exposes an increased length of the LEX leading-edge, which could affect the vortex flow above the LEX and the vortex breakdown position.

Fig.9 shows the vortex breakdown positions for four different combinations of leading- and trailing-edge flap deflections. The effects of flap settings appear to be minimal, and any variations that may occur are masked by the scatter of the results.

3.4 Effect of horizontal stabilator deflection

To reach and maintain the angles of attack at which vortex breakdown occurs, the horizontal stabilator of the F/A-18 must be deflected leading-edge downwards to generate the required pitching moment. The effect of such a control movement on the vortex breakdown axial position is shown in Fig.10, for an arbitrary stabilator deflection of -30^{0} (slightly greater than the maximum deflection of -24^{0} used in the actual aircraft). It is apparent that the stabilator deflection produces no measurable shift in the vortex breakdown position. For all the other 1/48 scale model tests described here, the stabilator angle was set to zero.

3.5 Effect of model scale and type

Some earlier measurements made on a 1/72 scale F/A-18 model are included here for comparison. The measurements were made in a vertical water tunnel and in a towing tank, using dye and hydrogen bubbles respectively for flow visualisation. The leading-edge/trailing-edge flap configuration was $20^{0}/20^{0}$, and the results are compared in Fig.11 with the results for the 1/48 scale model with a flap configuration of $35^{0}/35^{0}$. Once again, any variations within the results are masked by the scatter, further confirming that Reynolds number effects are not significant in measurements of this particular flow parameter.

Another factor of some concern in water tunnel testing using a hobby kit as the basis for the test model is the accuracy with which the kit represents the actual aircraft, and the likely effect on results of any inaccuracies in this representation. With the availability of two 1/48 scale models from two different sources (ARL - Monogram kit, Eidetics - Revell kit), the opportunity was taken to compare results of vortex breakdown position measurements on the two models.

The geometries of the models differed in several respects, and it was thought that these differences might cause variations in the position of vortex breakdown. Some of the model differences are illustrated in Fig.12. This diagram shows some comparative model cross-sections, obtained using a needle-type template former. It is thought that the ARL model is a more accurate representation of the full-scale aircraft, and the Eidetics model differs from the ARL model in several respects :

(a) the forward end of the LEX is set too high on the fuselage side;

(b) the undersurface of the LEX has dihedral, whereas the LEX undersurface on the full-scale aircraft has anhedral;

(c) the upper fuselage in the vicinity of the wing mid-chord is too flat;

(d) the engine inlets are too small.

Fig.13 shows a comparison between the vortex breakdown positions measured over the two models. It can be seen that despite the geometrical differences described above, there is good agreement between the two sets of results. Thus it appears that, at least in terms of the relatively crude parameter of axial position of vortex breakdown, changes in model cross-section shape of the type and scale described here have little effect on vortex behaviour. It is probable, however, that the model changes will have effects that are not apparent from flow visualisation tests of the type reported here. For example, small changes in forebody shape can have large effects on forebody pressure distributions (Ref.2) and hence on the yawing and pitching characteristics of the aircraft.

3.6 Effect of engine inlet flows

On the F/A-18, the engine inlets are located beneath the LEX/wing leading-edge junction, and it seemed possible that flow into the inlets might influence the behaviour of the vortex above the LEX in this region. Vortex breakdown positions were measured for various inlet flow rates, and the results are shown in Fig.14. The inlet flow rate is scaled using the ratio V_I/V_0, where V_I is the mean velocity through the inlet and V_0 is the freestream velocity. Examination of F/A-18 flight records showed that during a typical period of air combat manoeuvring, lasting for some 100 seconds at full throttle, the aircraft operated at angles of attack greater than 15^0 and at estimated inlet velocity ratios greater than 3.0 for more than 50% of the manoeuvring period. For nearly 20% of the period, the estimated velocity ratio exceeded 4.0, and the peak value was about 5.5. Fig.14 shows that the inlet flow does have an effect on the axial position of vortex breakdown, tending to shift it downstream. The downstream shift increases with inlet velocity ratio until, at a velocity ratio of 8.1, the shift is about 20% of the model length.

The effect of engine inlet flow is influenced by the leading-edge flap position, as shown in Fig.15. When the flap is undeflected, the downstream shift of the vortex breakdown is less than when the flap is deflected 35^0, at least for angles of attack between 20^0 and 35^0. This change is probably due to the reduction in the effective length of the LEX leading-edge exposed to the inlet flow effects when the flap is undeflected.

The effect of engine inlet flow on the overall flow structure in the LEX region was investigated in more detail by injecting dye through ports in the starboard fuselage side beneath the LEX and ahead of the inlets. The dye traces in this region will give a general idea of the local flow behaviour. However, details of the dye flow must be interpreted with care, as in this region of complex viscous flow, the appearance of the dye traces will be sensitive to the actual flow rate of the dye through the ports. Dye was also injected through a port beneath the LEX leading edge, outboard of the engine inlet.

Fig.16 shows dye patterns obtained for various inlet flow rates, at an angle of attack of 30.5^0. With no flow into the inlet, (Fig.16(a)), there is a region of complex flow beneath the LEX. Dye from the fuselage ports moves forward along the fuselage side to the LEX apex, up around the apex and into the LEX vortex core. Dye from the port beneath the LEX leading-edge moves outboard beneath the LEX, around the leading-edge and into the vortex system.

Under some conditions, the dye traces beneath the LEX indicate the formation of vortex-like structures in this region. A similar flow pattern was observed with a flow-through inlet (i.e. inlet open, suction system not connected). Similar regions of separated flow have been observed in wind tunnel tests[5], using surface flow visualisation. A panel method analysis[6] of the flow around the F/A-18, although carried out for a lower angle of attack, also indicated the presence of a separated flow region beneath the LEX when there was no flow into the inlet. Navier-Stokes solutions[7] to the flow around the F/A-18 forebody-LEX have indicated the presence of a vortex-like separation beneath the LEX at an angle of attack of 20^{0}.

For an inlet velocity ratio of 1.24, (Fig.16(a)), the extent of the separated-flow region beneath the LEX is reduced, and dye from the lowest port on the fuselage side moves downstream into the inlet splitter slot. The vortex breakdown position has shifted slightly downstream, and the vortex core upstream of the breakdown has been deflected downwards to lie roughly parallel to the LEX upper surface.

For a velocity ratio of 2.48, (Fig.16(b), the separated region beneath the LEX seems to have disappeared. Dye from all the fuselage side ports moves downstream and into the splitter slot or into the inlet itself. Relative to the V_I/V_0 = 1.24 case, the vortex breakdown has shifted slightly further downstream, while the point of downward deflection of the core upstream of the breakdown has remained in the same position relative to the model.

With further increase in inlet velocity ratio, the trends described above are continued. For a velocity ratio of 4.96, (Fig.16(b)), more dye from the fuselage side ports passes directly into the inlets, and the vortex breakdown position has shifted further downstream. Some dye from the port beneath the LEX leading-edge is also sucked inboard beneath the LEX and into the inlet. For a velocity ratio of 8.1, (Fig.16(c)), more dye from this port is sucked into the inlet. At high inlet flow rates, observation of hydrogen bubbles generated along the LEX leading-edge indicates that, just ahead of this dye port, the normal upward flow around the LEX leading-edge does not occur. In fact, fluid passes down around the LEX leading-edge from the upper to the lower surface.

The effect of inlet flow at an inlet velocity ratio of 8.1 at other angles of attack is shown in Fig.17. At an angle of attack of 19.5^{0}, (Fig.17(a) and (b)), the vortex core is deflected inboard and the vortex breakdown has shifted from a position just ahead of and outboard of the fin leading-edge at $V_I/V_0 = 0$, to a position behind and inboard of the leading-edge. At an angle of attack of 25.4^{0}, (Fig.17(c) and(d)), the corresponding shift in vortex breakdown position is from just aft of the wing leading-edge / LEX junction to just ahead of the fin leading-edge. Even at an angle of attack of 40.3^{0}, (Fig.17(g) and (h), where vortex breakdown occurs well forward of the inlet location, inlet flow has some effect on the breakdown position.

Flow into the engine inlet, by modifying the flow patterns beneath the LEX, may be causing local changes to the effective spanwise camber of the LEX. Thus when the inlet flow is zero or very small, the separated region below the LEX "fills out" the space between the LEX lower surface and the fuselage side, giving an effective negative spanwise camber to the LEX. As the inlet flow increases, the separated region is reduced and eventually largely disappears. This process makes the effective spanwise camber of the LEX more positive. It has been shown in wind tunnel[8] and water tunnel[9] tests that increasing the spanwise camber of a delta wing shifts the vortex breakdown position downstream. It is possible that a similar mechanism is producing the results observed for the LEX vortex in the present tests.

The effect of inlet flow on the position of vortex breakdown may be significant in relation to wind tunnel testing. Most wind tunnel tests of the F/A-18 have been performed using flow-through inlets. The water tunnel tests described here have shown that flow-through inlets give the same results as inlets with no flow through them. The internal inlet duct flow conditions in the water tunnel model are likely to differ considerably in geometry and Reynolds number from those in a typical wind tunnel model with flow-through inlets. However, if the water tunnel results can be assumed to apply at all under wind tunnel test conditions, it would appear necessary to simulate inlet flows to model accurately the behaviour of LEX vortex breakdown in the wind tunnel. Appropriate comparative wind tunnel tests are needed to check on this point.

Another aspect of inlet flow effects concerns the apparent good agreement between measurements of vortex breakdown position made in the water tunnel and those made in flight (Fig.8). The water tunnel measurements in Fig.8 were made with no inlet flow, while the flight measurements would have been made with engines running, probably at a quite high thrust level. The agreement between flight results and water tunnel results with inlet flow simulation would be much less close than that shown in Fig.8. This aspect requires further investigation to clarify the extent of inlet flow effects and their Reynolds number dependence. Wind tunnel tests with simulated inlet flows would be one approach. Also, it would be informative to have accurate estimates of actual inlet velocity ratios under flight conditions.

3.7 Effect of airbrake deployment

On the F/A-18, the airbrake is mounted on the fuselage upper surface between the vertical fins. The airbrake is hinged at its forward edge, and is deflected upwards into the airstream when deployed. The deflected airbrake represents a considerable blockage to the flow between the fins, and it was of interest to see if this blockage had any effect on the position of vortex breakdown.

Fig.18 shows the results of vortex breakdown position measurements with the airbrake deflected upwards at an angle of about 60°. It appears that the airbrake has little or no effect on the vortex breakdown axial position for most of the angle of attack range. At the lower angles of attack, there may be some slight downstream movement of the breakdown, but this movement is little greater than the experimental scatter.

3.8 Effect of LEX fences

3.8.1 Vortex breakdown position

The fitting of the LEX fences has little effect on the vortex breakdown axial position, as can be seen from the results plotted in Fig.19. However, the fences do modify the vortex system structure to some extent, particularly at angles of attack in the range 15° - 30°. Fig.20 shows comparative fence-off and fence-on side and plan views for various angles of attack. At an angle of attack of 19.5°, (Fig.20(a) and (b)), the fence causes the development of a slight spiral in the vortex core, which is deflected initially upward and inboard, then downward and outboard. The breakdown itself is shifted outboard slightly.

For angles of attack up to about 27°, with breakdown occurring close to or downstream of the fence position, the physical appearance of the breakdown is altered by the addition of the fences. With the fences off, the breakdown is clearly defined as a sudden deformation and expansion of the core dye filament. With the fences fitted, the breakdown appears less distinct, with a more gradual thickening of the core dye filament upstream of the breakdown proper (Fig.20(a) and (c)).

At an angle of attack of 25.4°, (Fig.20(c) and (d)), the vortex core kink caused by the fence is still present but is less apparent than at the lower angle of attack. At an angle of attack of 30.5°, Fig.20(e) and (f), the vortex breakdown is occurring in the vicinity of the fence position, and the fence does not appear to have much effect on the shape of the vortex core.

Thus it appears that the favourable effect on fin dynamic loading produced by the fences is not the result of any major axial shift in vortex breakdown position, but rather is due to a change in the nature of the flow downstream of the breakdown, combined with a slight lateral shift in the position of the breakdown, at least at the lower angles of attack.

Fig.21 shows that the effect of inlet flow on vortex breakdown position with the fences on is similar to the effect with fences off. The process by which inlet flow displaces the vortex breakdown downstream does not appear to be markedly affected by the presence of the fences.

3.8.2 Fence effects on LEX vortex

Wind tunnel tests[2] and flight tests[3] have shown that the fitting of the LEX fences has a favourable effect on the fin vibration levels. The tests discussed above indicate that the axial position of the vortex breakdown is not greatly affected by the fence, so some more detailed flow visualisation tests were carried out in an attempt to understand how the fence works.

To provide more information on the behaviour of the flow in the vicinity of the fence, the hydrogen bubble technique was used, in conjunction with laser sheet illumination. In a typical case, Fig.22 shows successive sections through the hydrogen bubble sheets as the light sheet is moved downstream past the fence location. Well upstream of the fence, the vortex cross section is typical of that above a delta wing. The sheet of fluid separating from the leading edge rolls up smoothly into a spiral vortex above the LEX and inboard of the leading edge. Further downstream, in the vicinity of the fence, a kink develops in the separated sheet. This kink develops into a second vortex, of the same sense as the main LEX vortex. The second vortex moves inboard and upwards over the main vortex, then downwards on the inboard side of the main vortex. Ultimately, the two vortices merge. The interaction between the two vortices accounts for the kinks that develop in the LEX vortex core upstream of the breakdown when the fences are fitted, and also for the slight outboard displacement of the LEX vortex core.

The behaviour of the two vortices is similar to that which occurs over double delta wings[10], where a second vortex generated by the kink in the leading edge interacts with the vortex from the wing apex. Fig.23 shows a possible topology of the cross flow streamlines in the vicinity of the LEX fence. This is similar in many respects to the cross-flow topology over a double-delta wing (Fig.30, Ref.10). A saddle point is present between the main LEX vortex and the second vortex caused by the presence of the fence.

The interaction of the two vortices may affect the frequency of any unsteady flow component downstream of the breakdown, and may thus contribute to the effectiveness of the fences in reducing fin vibration. The techniques used in the flow visualisation tests described here did not allow the detection of any such frequency changes.

The occurrence of a second vortex caused by the presence of the fence was observed by Erickson et al[2] in wind-tunnel tests, using smoke to make the vortex cores visible. The general behaviour of the LEX main vortex and the fence-induced vortex observed in the wind tunnel tests closely matches the water tunnel results discussed here.

When attempting to measure the vortex breakdown position with fences on, it was found that, for a small angle of attack range, the breakdown was not clearly defined by dye injected at the LEX apex. The dye filament in the vortex core appeared to deflect and spread out into a curved sheet, without displaying the usual clearly defined stagnation point at breakdown.

To study this flow in more detail, dye was injected through a hole on the LEX underside at about the same chordwise position as the fence. This dye passed outboard beneath the LEX, upwards around the LEX leading-edge and into the second vortex. Dye was also injected through a hole on the LEX upper surface upstream of the fence. Dye from this hole passed downstream over the LEX upper surface and into the second vortex. Some examples of the flow patterns observed are shown in Fig.24. It was found that the principal breakdown was in fact occurring in the second vortex, and that the deflection and spreading of the main vortex core dye was due to the core deflecting and "smearing" around the breakdown in the second vortex. This flow pattern was observed clearly at relatively low flow velocities (about 30 mm/s), and for an angle of attack range of about 17^{o} - 22^{o}. At higher velocities, diffusion and mixing of the dye filaments made it impossible to distinguish which vortex broke down first. However, breakdown of the second vortex may account for the change in appearance of the LEX vortex breakdown caused by the fitting of the fence.

4.0 CONCLUDING REMARKS

The experimental measurements described in this report have shown that, within the limits of the accuracy of the flow visualisation techniques used, the axial position of breakdown in the F/A-18 LEX vortex is insensitive to a number of parameters, including Reynolds number, flap setting, stabilator deflection, airbrake deployment, variations in LEX cross-sectional shape, and the fitting of LEX fences. Fig.25 shows a plot of all the results obtained in these tests with zero inlet flow, plus results obtained from wind tunnel tests and flight tests. The results all fall within a band that is little wider than that due to experimental scatter. Vortex breakdown positions from the wind tunnel and flight tests tend to fall on the upstream edge of the plotted group.

The simulation of engine inlet flows affected the axial position of vortex breakdown, at inlet flow velocity ratios that could be encountered in practical flight conditions at high angles of attack, low airspeeds and high thrust settings. Basically, as the ratio of engine inlet flow velocity to freestream velocity increased, the breakdown position moved downstream. Results for one inlet velocity ratio are included in Fig.25.

The effects of inlet flow require further investigation, by wind tunnel tests using inlet flow simulation, rather than using only flow-through inlets. It appears that the good agreement between water tunnel and flight test measurements of vortex breakdown axial position may be adversely affected by the inclusion of inlet flow effects.

The addition of LEX fences, while not producing a significant shift in the axial position of LEX vortex breakdown, did modify the LEX vortex structure. The fitting of the fence caused the formation of a second vortex originating from the LEX leading-edge near the fence. Apparently it is the interaction between this vortex and the main LEX vortex that produces the favourable reduction in fin vibration reported from wind tunnel and flight tests.

ACKNOWLEDGEMENTS

The author would like to acknowledge with thanks the useful discussions which he had with Dr B.D. Fairlie and Mr C.A Martin of Flight Mechanics Branch ARL during the course of this work.

REFERENCES

1.	Erickson, G.E.	*Water tunnel flow visualisation and wind tunnel data analysis of the F/A-18* NASA CR 165859 (May 1982)
2.	Erickson, G.E. Hall, R.M. Banks, D.W. DelFrate, J.H. Schreiner, D.A. Hanley, R.J. Pulley, C.T.	*Experimental investigation of the F/A-18 vortex flows at subsonic through transonic speeds* AIAA 7th Applied Aerodynamics Conf., 31 Jul - 2 Aug. 1989, Seattle, Washington Paper AIAA-89-2222
3.	Lee, B.H.K. Brown, D. Zgela, M. Poirel, D.	*Wind tunnel investigation and flight tests of tail buffet on the CF-18 aircraft* AGARD Specialists' Meeting on Aircraft Loads due to Flow Separation, Sorrento, Italy, 1-6 April, 1990. Paper 1.
4.	Wentz, W.H.	*Vortex-fin interaction on a fighter aircraft* AIAA 5th Applied Aerodynamics Conference, Monterey, 17-19 Aug., 1987 Paper AIAA-87-2474
5.	Banks, D.W.	*Wind-tunnel investigation of the forebody aerodynamics of a vortex-lift fighter configuration at high angles of attack* SAE Paper 881419 (1988)
6.	Toffoletto, R.	*Development of a VSAERO model of the F/A-18* ARL Flight Mechanics TM 404 (Mar 1989)
7.	Ghaffari, F. Luckring, J.M. Thomas, J.L. Bates, B.L.	*Navier-Stokes solutions about the F/A-18 forebody-LEX configuration* AIAA 27th Aerospace Sciences Mtg., 9-12 Jan., 1989, Reno, Nevada Paper AIAA-89-0338

8. Earnshaw, P.B.
Lawford, J.A.
Low-speed wind-tunnel experiments on a series of sharp-edged delta wings
ARC R&M 3424 (1966)

9. Thompson, D.H.
A water tunnel study of vortex breakdown over wings with highly swept leading edges
ARL Aerodynamics Note 356 (May, 1975)

10. Thompson, D.H.
A visualisation study of the vortex flow around double-delta wings
ARL Aerodynamics Report 165 (Aug.,1985)

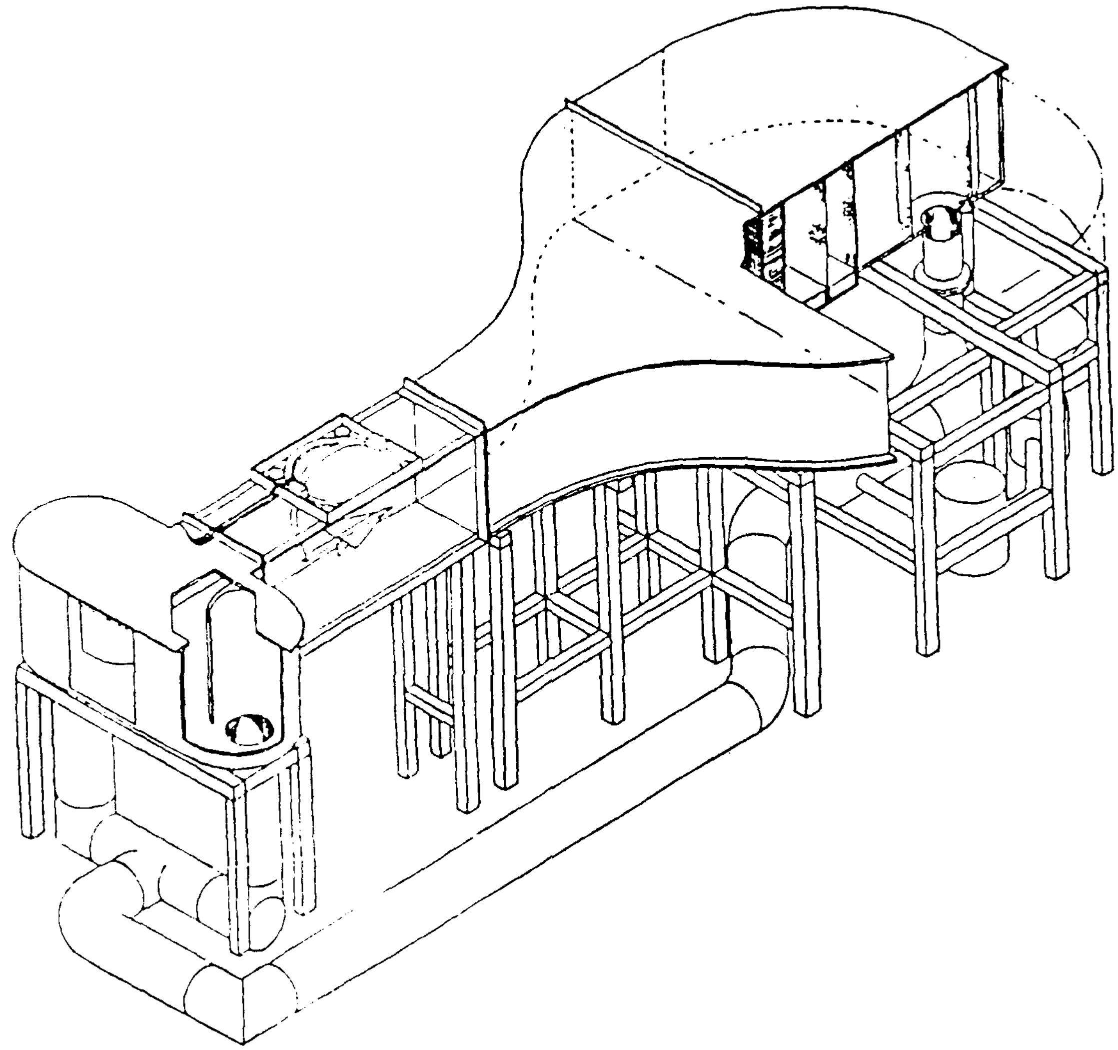

Fig.1 ARL Flight Mechanics Branch Water Tunnel

(Eidetics Model 1520)

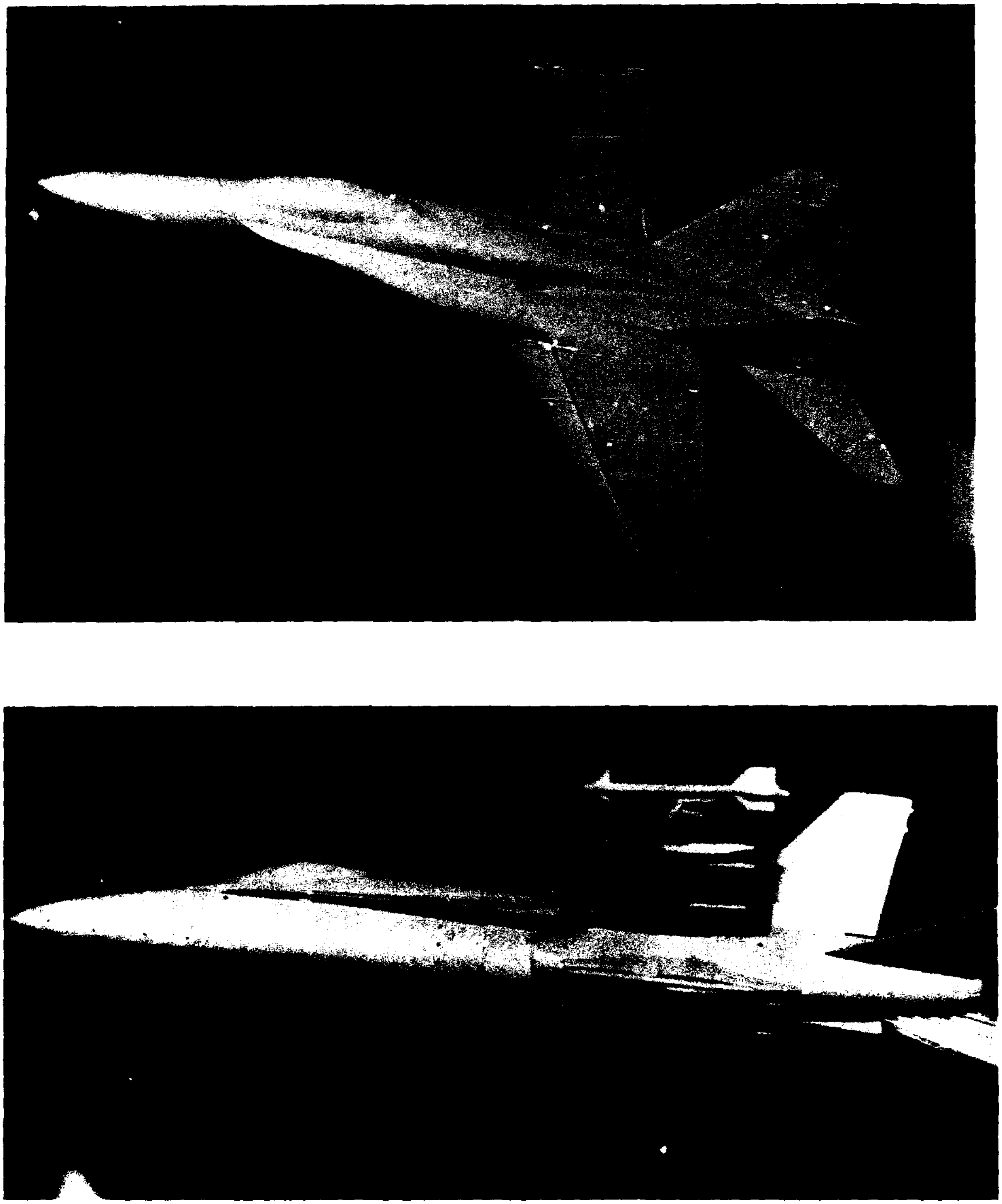

Fig.2 1/48 scale F/A-18 model

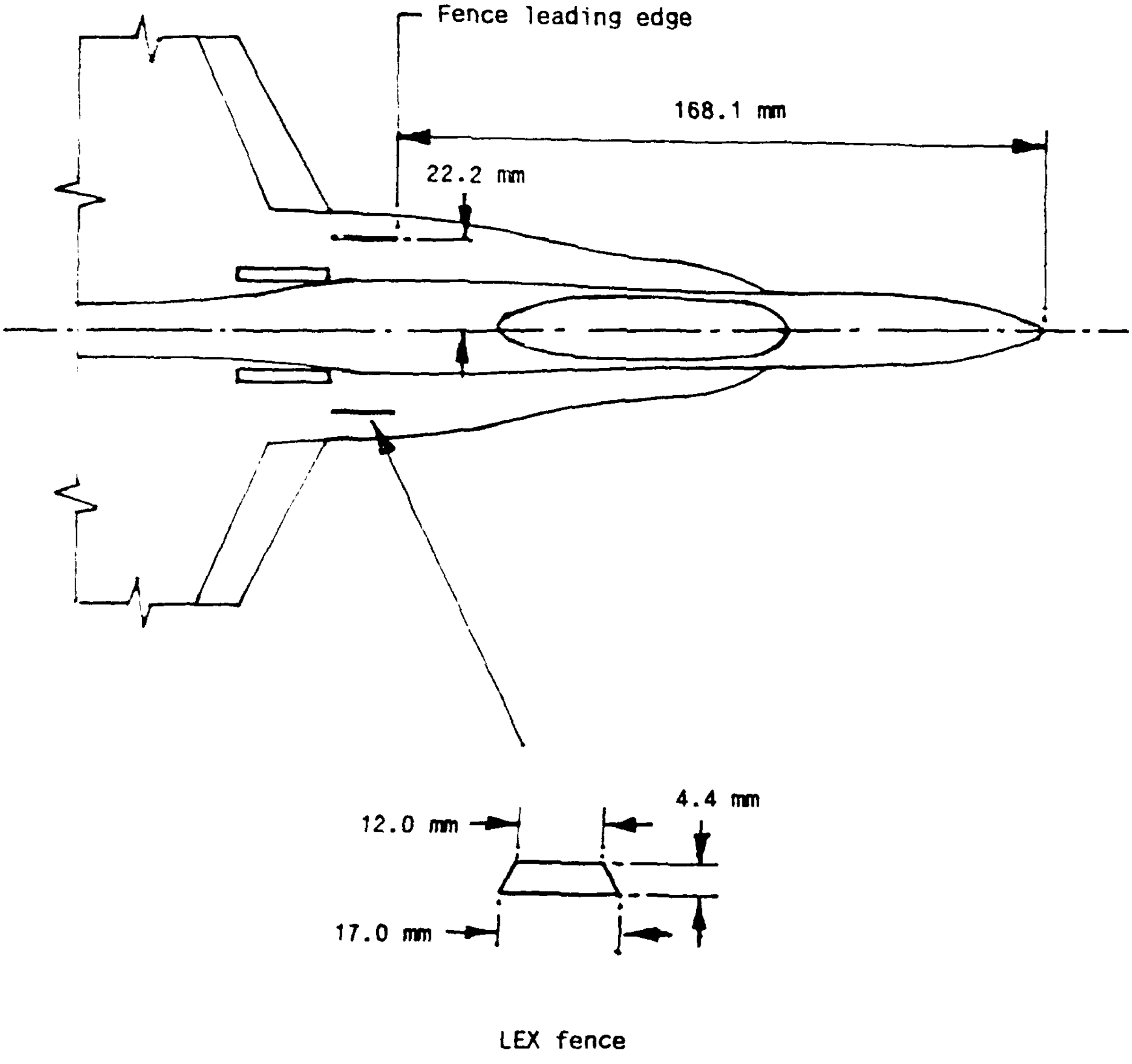

Fig.3 Shape and position of LEX fence on 1/48 scale model

Fig.4 Sample print from video copy processor

Fig.5(a) Vortex flow over F/A-18 - Reference configuration
Angle of attack = 19.5^{o}
(LEF/TEF = 35^{o}/0^{o}; V_{o} = 80 mm/s; LEX fences off; V_I/V_o = 0)

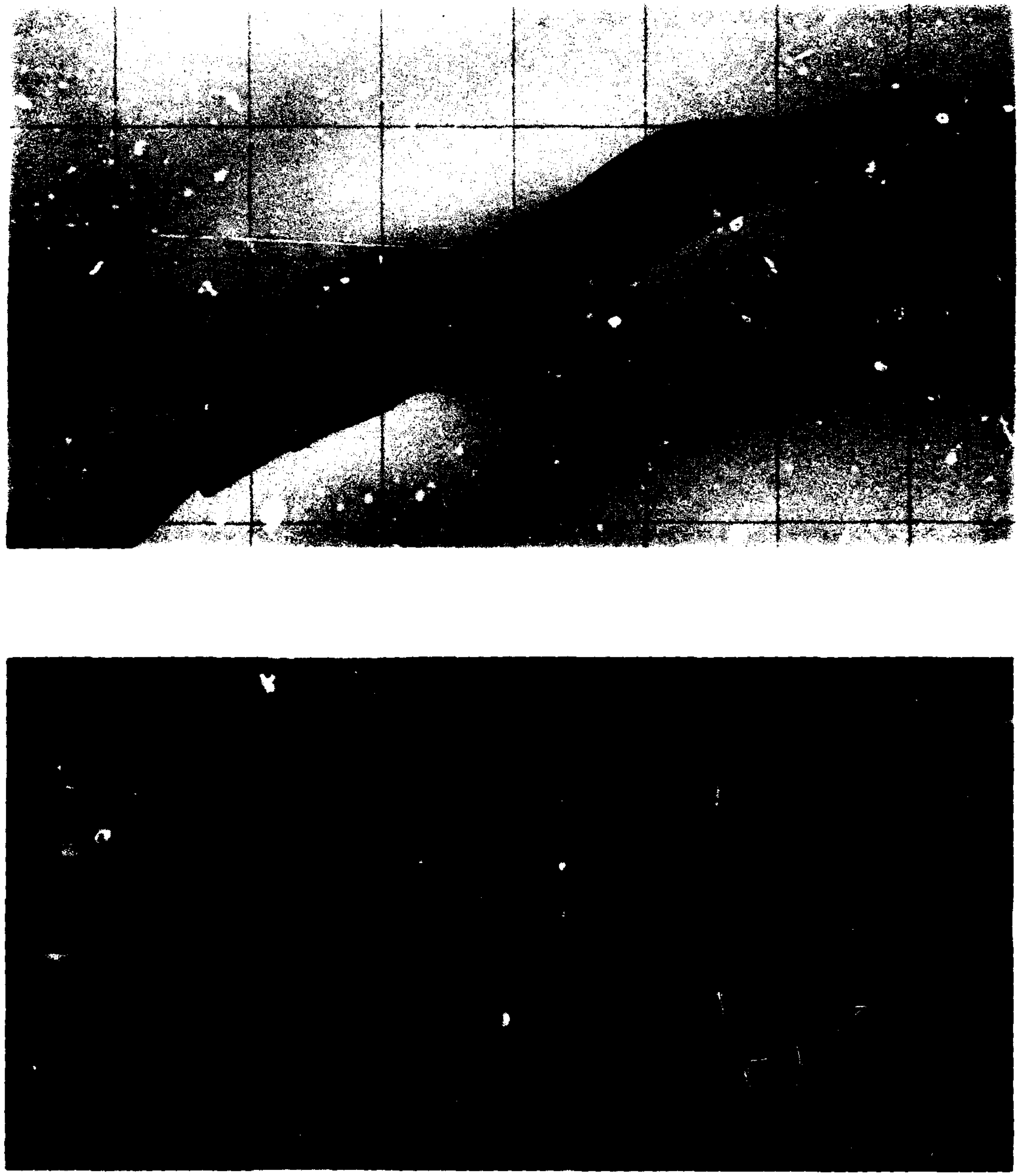

Fig.5(b) Vortex flow over F/A-18 - Reference configuration

Angle of attack = 25.4^{o}

(LEF/TEF = $35^{o}/0^{o}$; V_{o} = 80 mm/s; LEX fences off; V_{I}/V_{o} = 0)

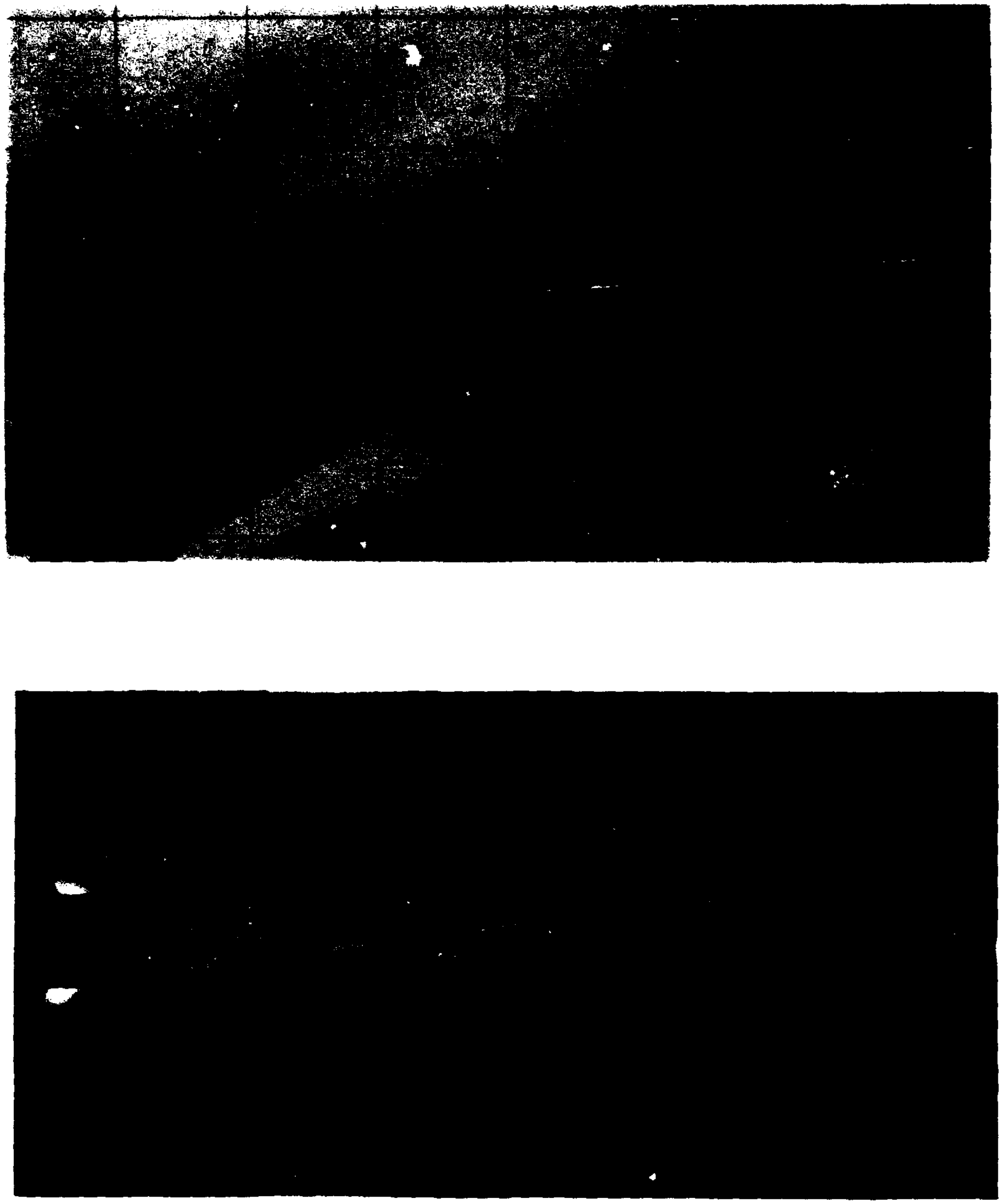

Fig.5(c) Vortex flow over F/A-18 - Reference configuration

Angle of attack = 30.5^{o}

(LEF/TEF = $35^{o}/0^{o}$; V_{o} = 80 mm/s; LEX fences off; V_{I}/V_{o} = 0)

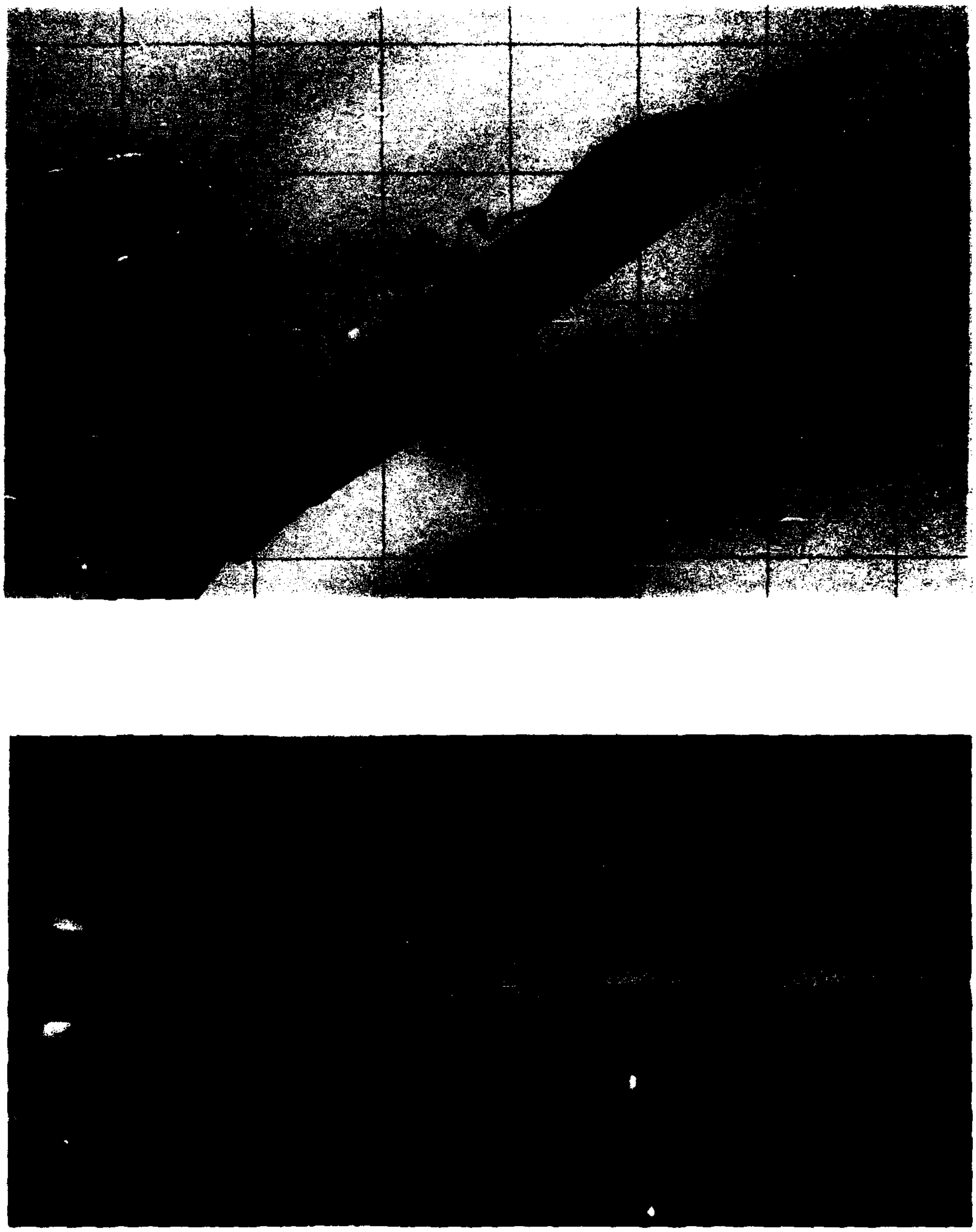

Fig.5(d) Vortex flow over F/A-18 - Reference configuration

Angle of attack = 35.5^{o}

(LEF/TEF = 35^{o}/0^{o}; V_o = 80 mm/s; LEX fences off; V_I/V_o = 0)

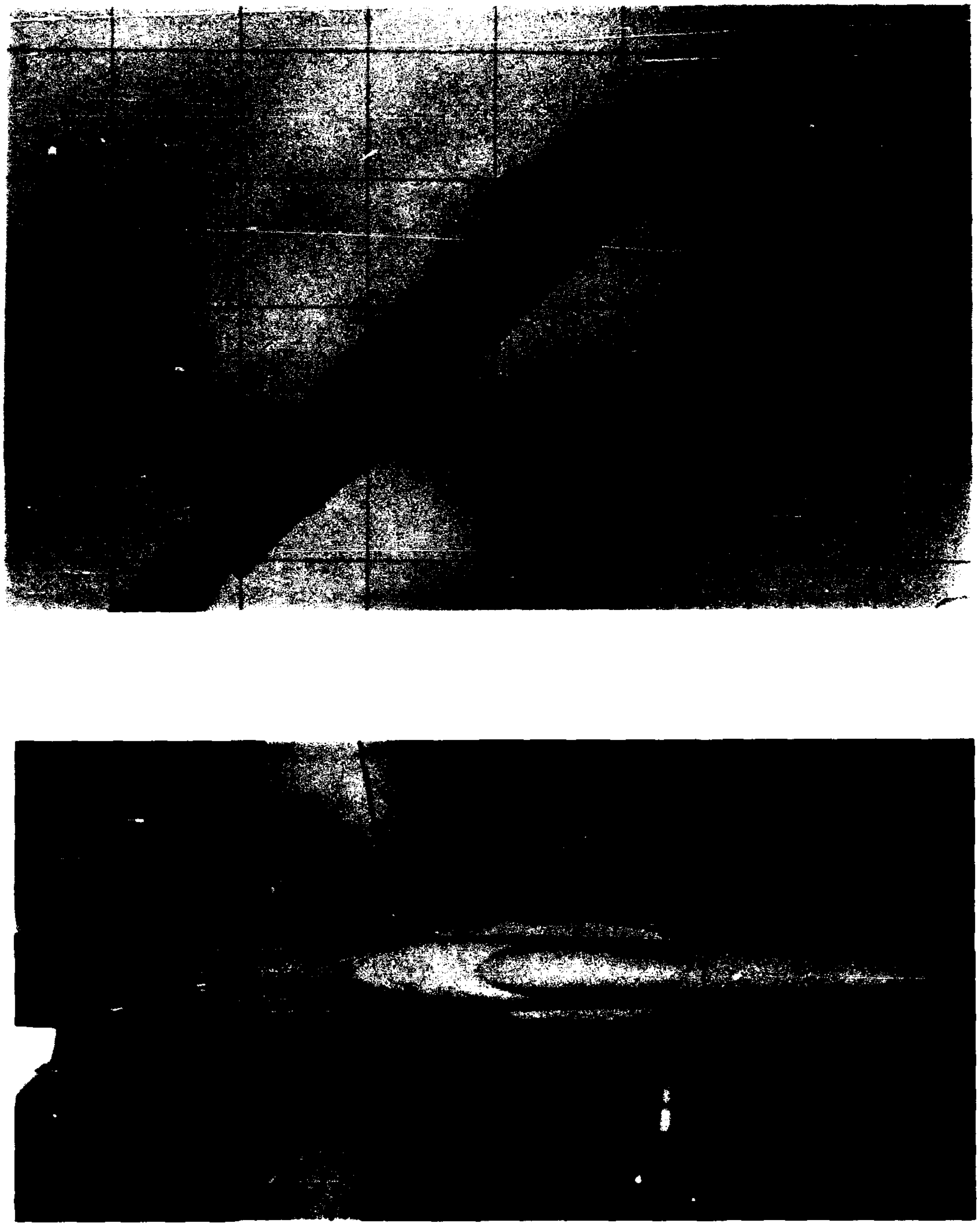

Fig.5(e) Vortex flow over F/A-18 - Reference configuration

Angle of attack = 40.3^{o}

(LEF/TEF = $35^{o}/0^{o}$; V_{o} = 80 mm/s; LEX fences off; V_I/V_o = 0)

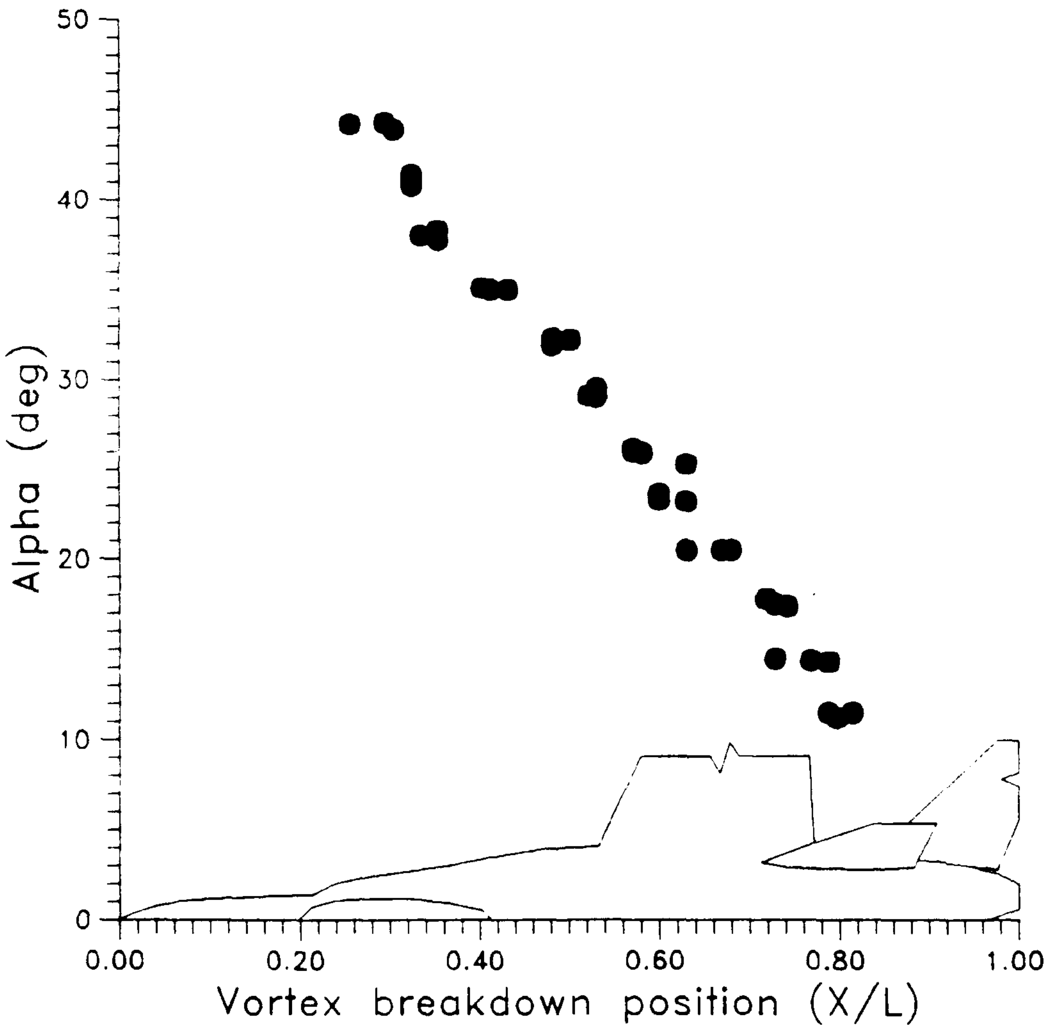

Fig.6 Vortex breakdown position over F/A-18.

Reference configuration.

(LEF/TEF = $35^{o}/0^{o}$; V_{o} = 80 mm/s; LEX fences off; V_{I}/V_{o} = 0)

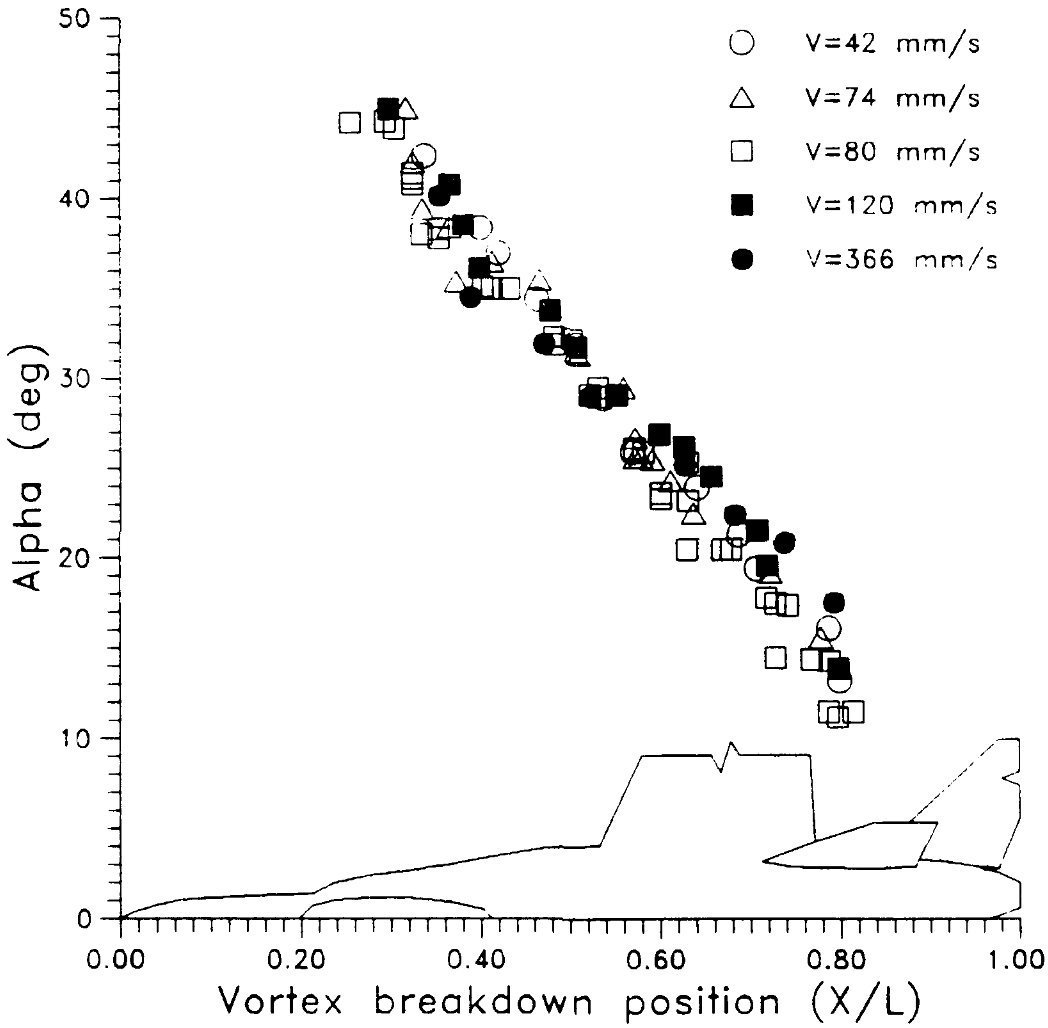

Fig.7 Vortex breakdown position over F/A-18
Effect of flow velocity
(LEF/TEF = $35^{o}/0^{o}$; LEX fences off; V_I/V_O = 0)

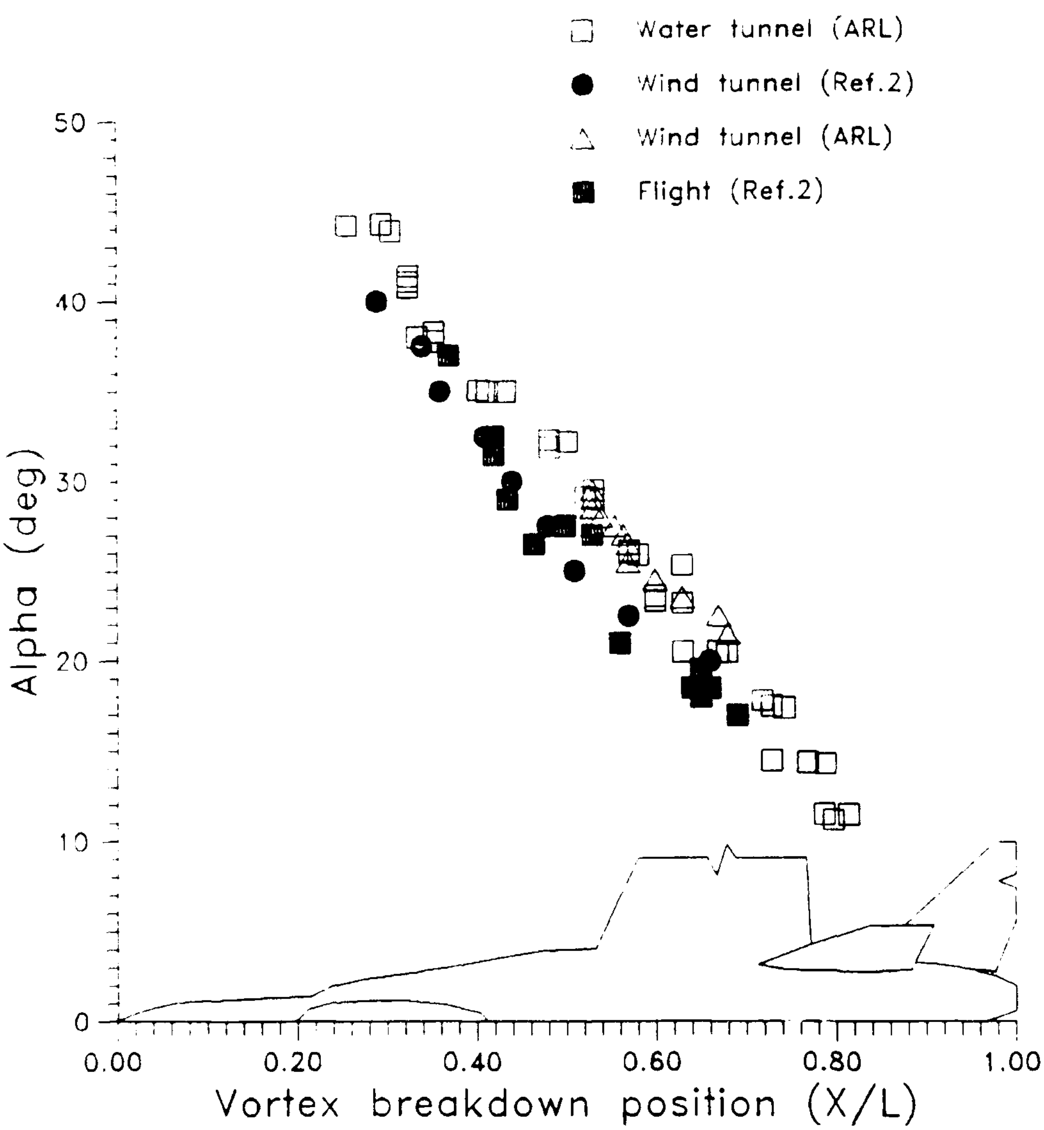

Fig.8 Vortex breakdown position over F/A-18
Comparison of water tunnel,
wind tunnel and flight test results

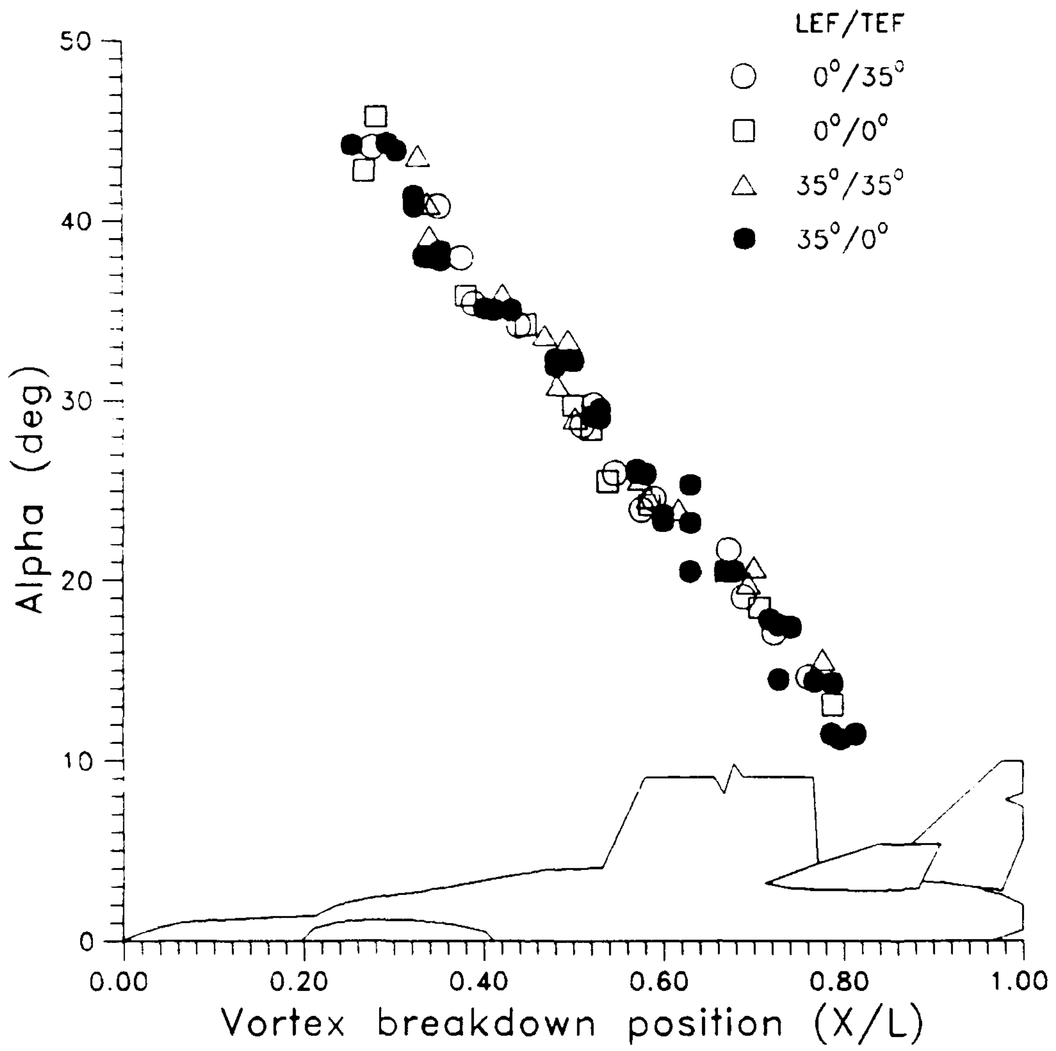

Fig.9 Vortex breakdown position over F/A-18

Effect of flap settings

(V_O = 80 mm/s; LEX fences off; V_I/V_O = 0)

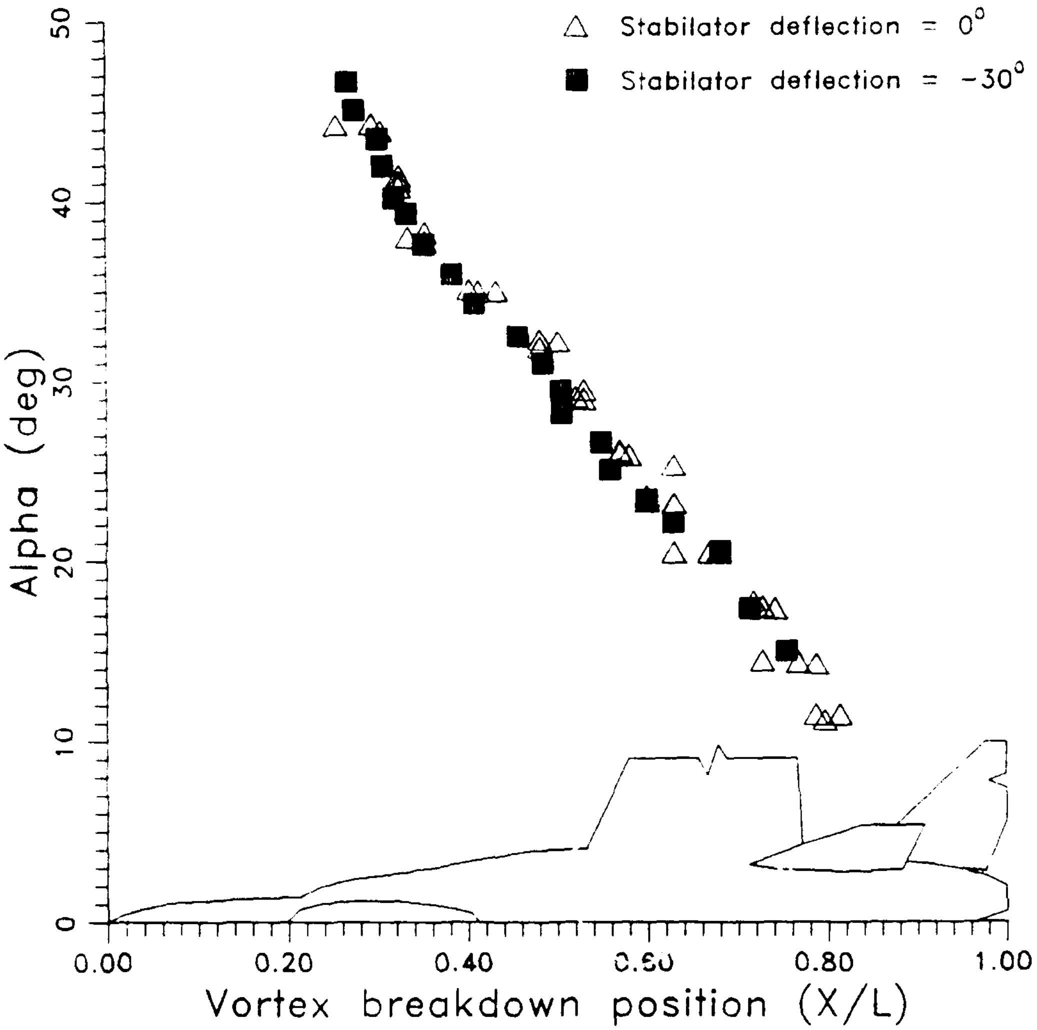

Fig.10 Vortex breakdown position over F/A-18

Effect of stabilator deflection

(LEF/TEF = $35^{o}/0^{o}$; V_{o} = 80 mm/s; LEX fences off; V_{I}/V_{o} = 0)

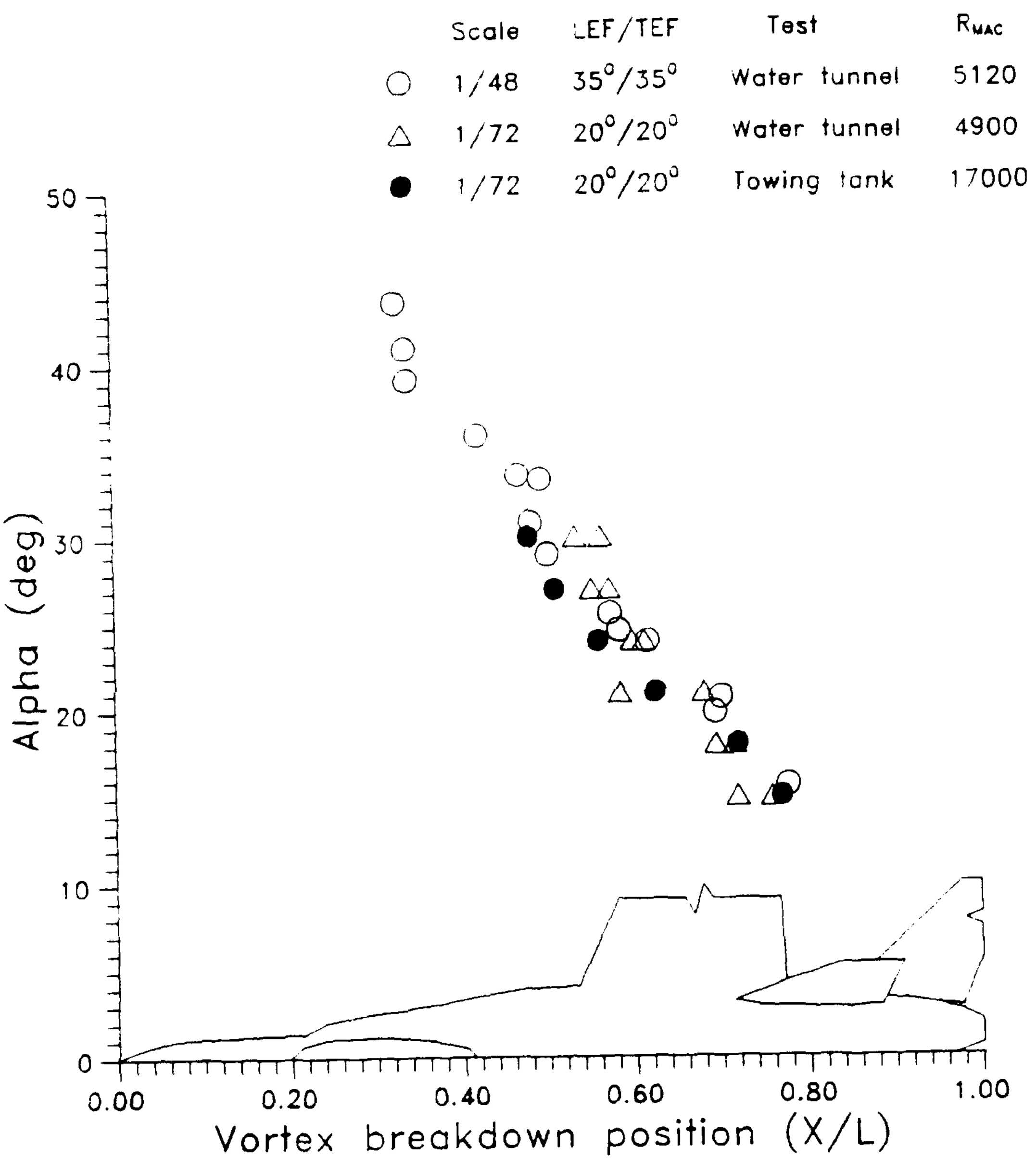

Fig.11 Vortex breakdown position over F/A-18
Results for models of different scales

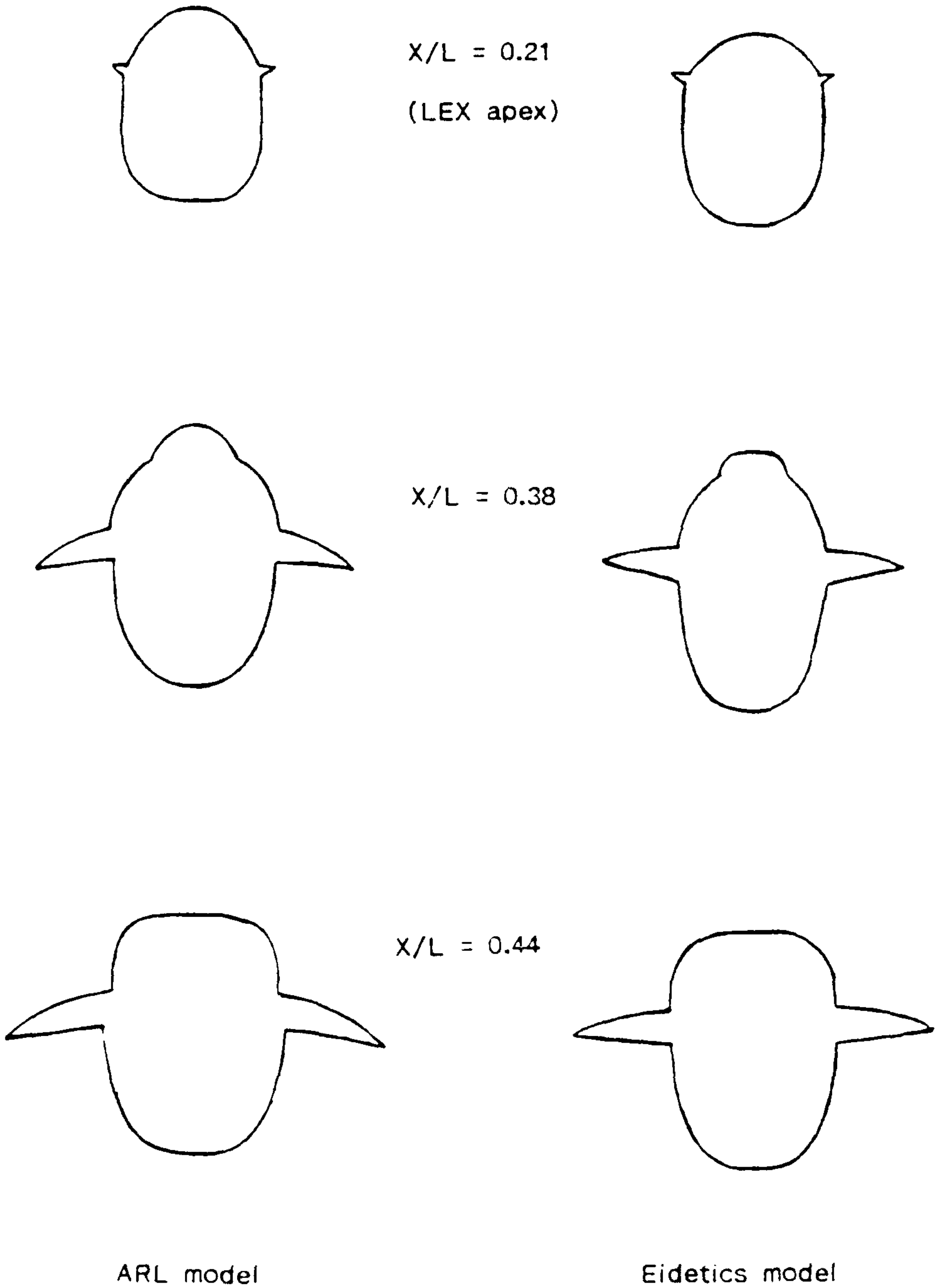

Fig.12 Differences between Eidetics and ARL 1/48 scale models

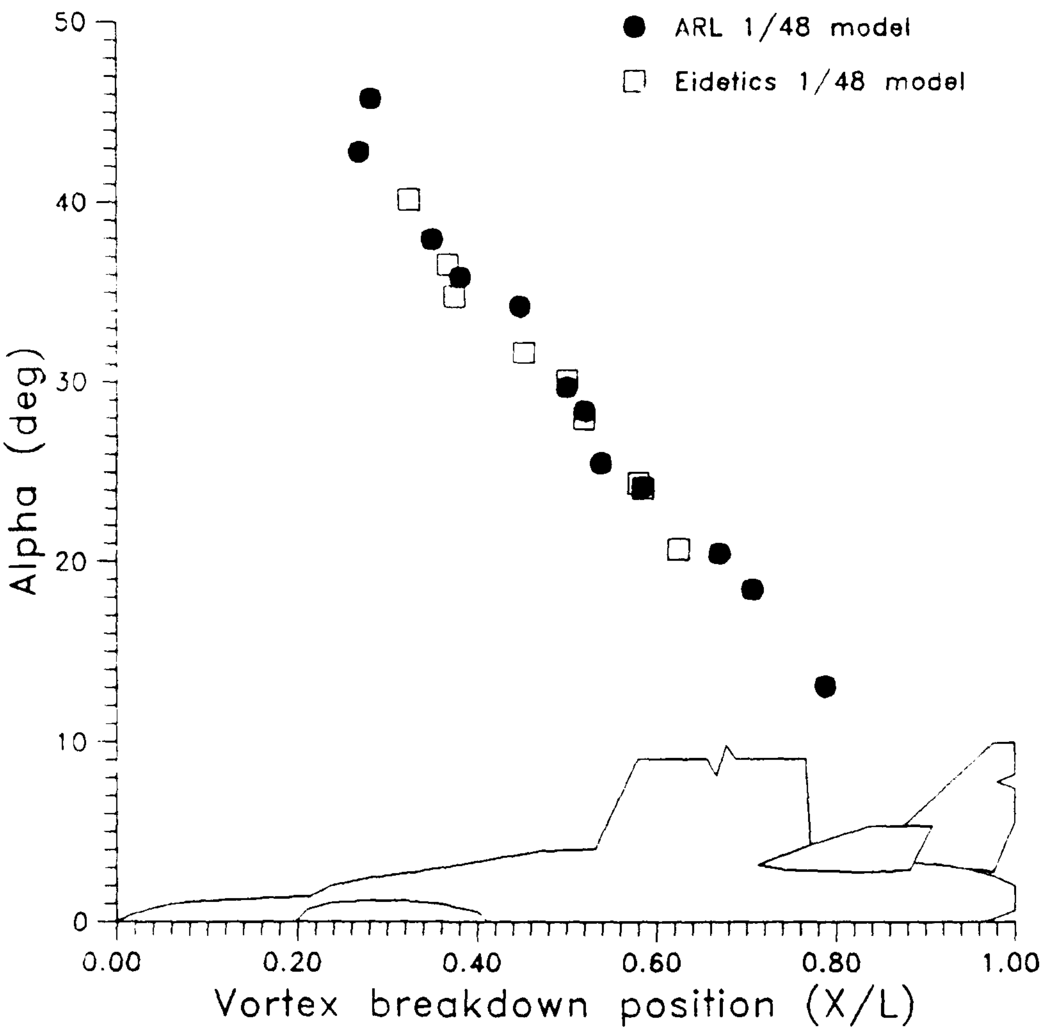

Fig.13 Vortex breakdown position over F/A-18
Results for different 1/48 scale models
(LEF/TEF = $0^o/0^o$; V_o = 80 mm/s; LEX fences off; V_I/V_o = 0)

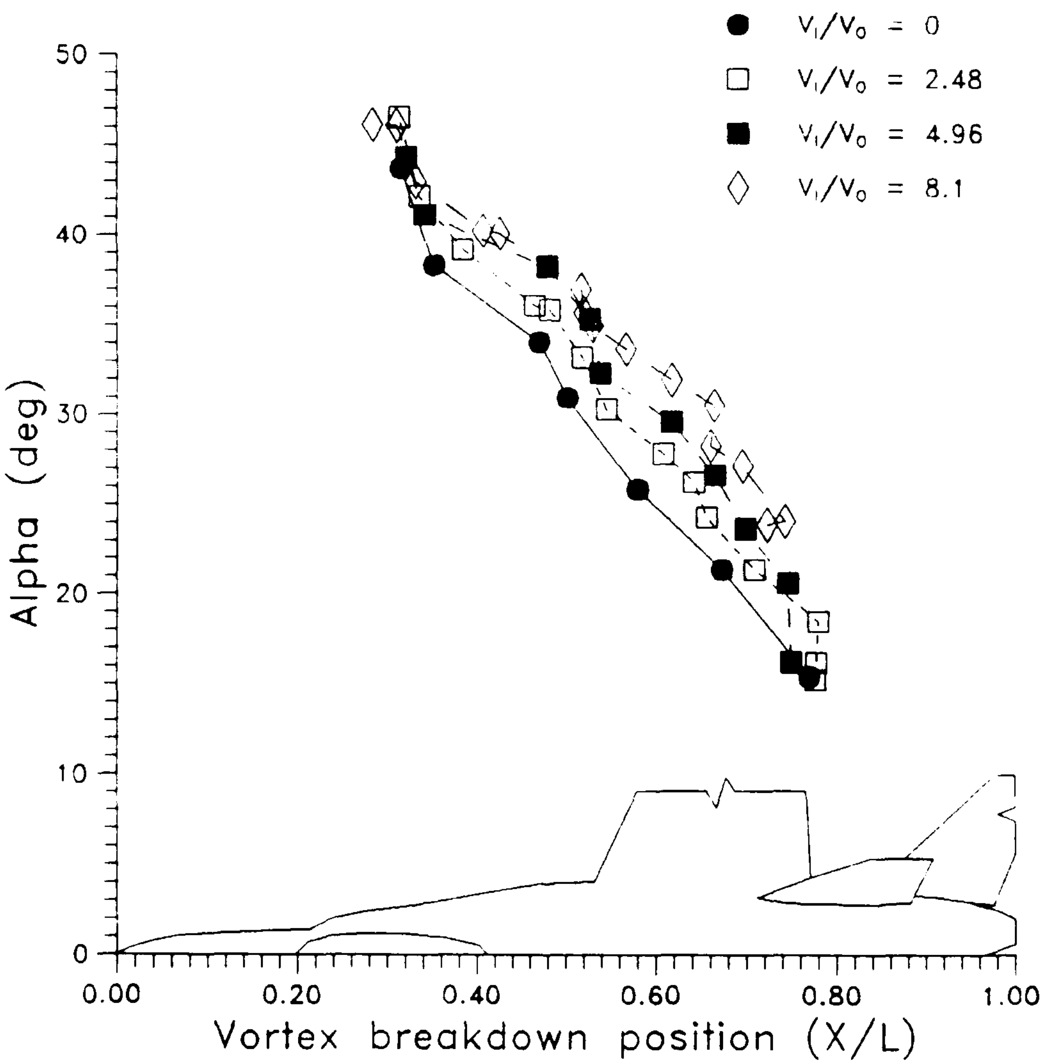

Fig.14 Vortex breakdown position over F/A-18

Effect of engine inlet flow

(LEF/TEF = $35^o/0^o$; V_o = 80 mm/s; LEX fences off)

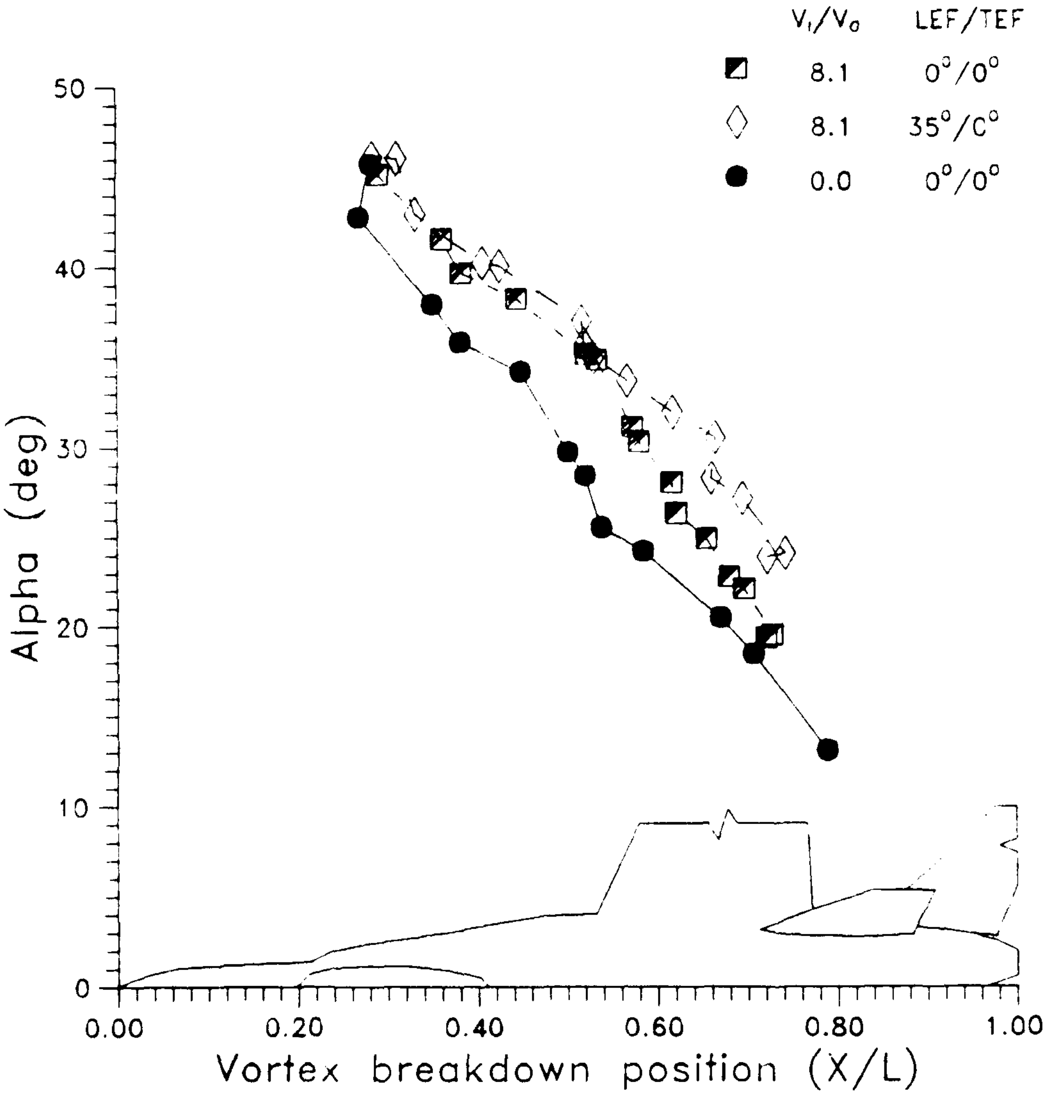

Fig 15 Vortex breakdown position over F/A-18
Effect of engine inlet flow at different flap settings
(V_O = 80 mm/s; LEX fences off)

$V_I/V_O=0$

$V_I/V_O=1.24$

Fig.16(a) Vortex flow patterns over F-18 - Effect of engine inlet flow
V_I/V_o = 0.0, 1.24
(Angle of attack = 30.5^o; LEF/TEF = 35^o/0^o; V_o = 80 mm/s; LEX fences off)

V_I/V_O=2.48

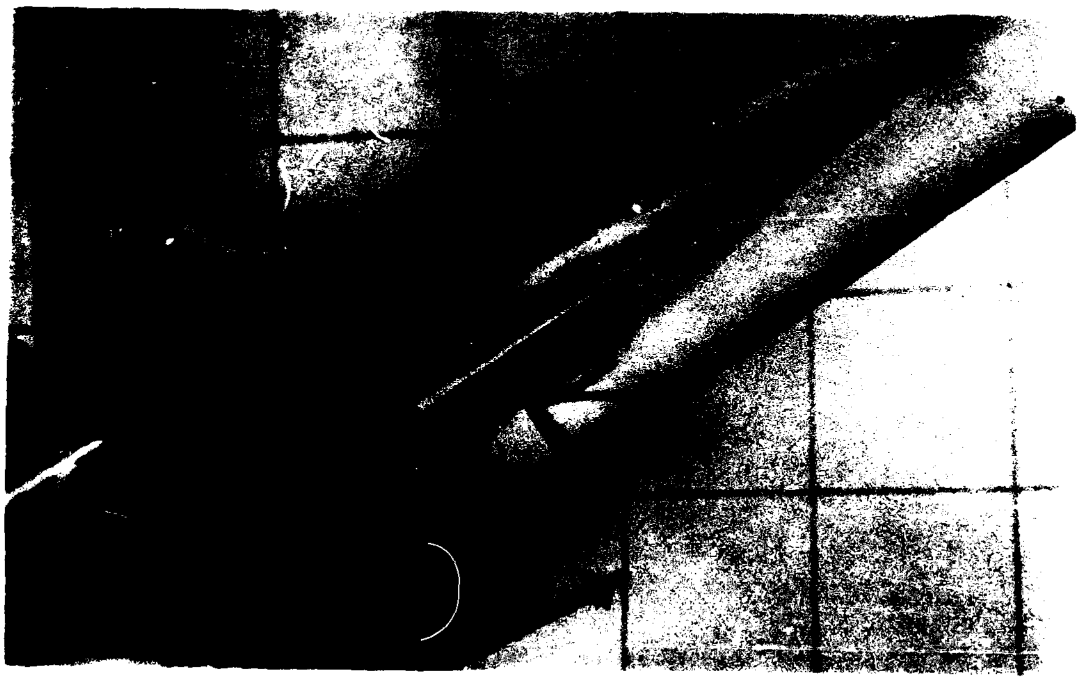

V_I/V_O=4.96

Fig.16(b) Vortex flow patterns over F-18 - Effect of engine inlet flow
V_I/V_o = 2.48, 4.96
(Angle of attack = 30.5^o; LEF/TEF = $35^o/0^o$; V_o = 80 mm/s; LEX fences off)

$V_I/V_O = 8.1$

Fig.16(c) Vortex flow patterns over F-18 - Effect of engine inlet flow

$V_I/V_o = 8.1$

(Angle of attack = 30.5^o; LEF/TEF = $35^o/0^o$; V_o = 80 mm/s; LEX fences off)

$V_I/V_O=0$

$V_I/V_O=8.1$

Fig.17(a) Effect of inlet flow at different angles of attack

Angle of attack = 19.5^o (Side view)

(LEF/TEF = $35^o/0^o$; V_o = 80 mm/s; LEX fences off)

$V_I/V_O=0$

$V_I/V_O=8.1$

Fig.17(b) Effect of inlet flow at different angles of attack
Angle of attack = 19.5^{o} (Plan view)
(LEF/TEF = 35^{o}/0^{o}; V_o = 80 mm/s; LEX fences off)

$V_I/V_O=0$

$V_I/V_O=8.1$

Fig.17(c) Effect of inlet flow at different angles of attack
Angle of attack = 25.4^o (Side view)
(LEF/TEF = 35^o/0^o; V_o = 80 mm/s; LEX fences off)

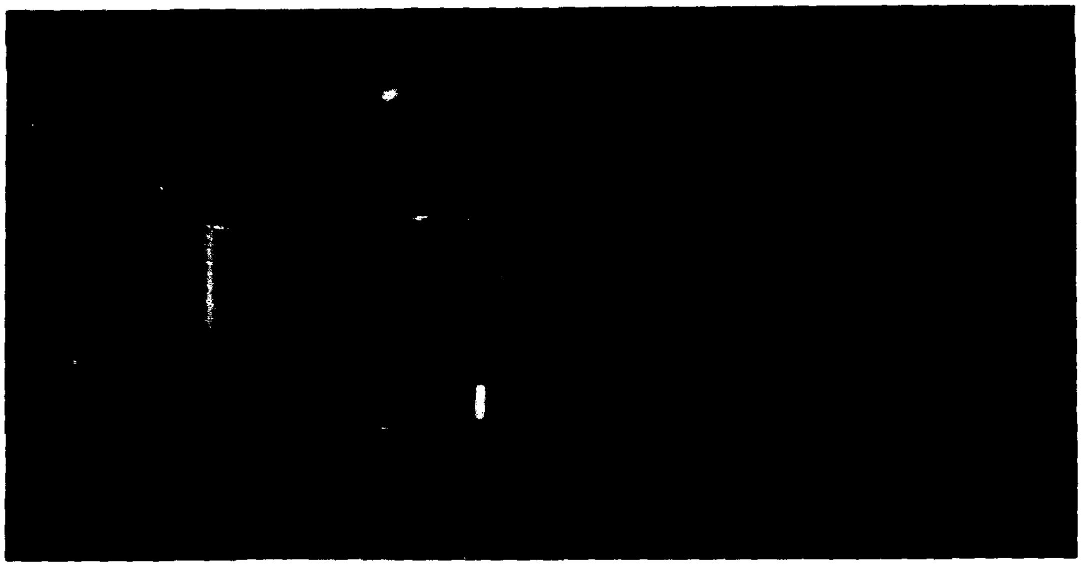

$V_I/V_O=0$

$V_I/V_O=8.1$

Fig.17(d) Effect of inlet flow at different angles of attack
Angle of attack = 25.4^{o} (Plan view)
(LEF/TEF = 35^{o}/0^{o}; V_o = 80 mm/s; LEX fences off)

$V_I/V_O=0$

$V_I/V_O=8.1$

Fig.17(e) Effect of inlet flow at different angles of attack
Angle of attack = 30.5^O (Side view)
(LEF/TEF = 35^O/0^O; V_O = 80 mm/s; LEX fences off)

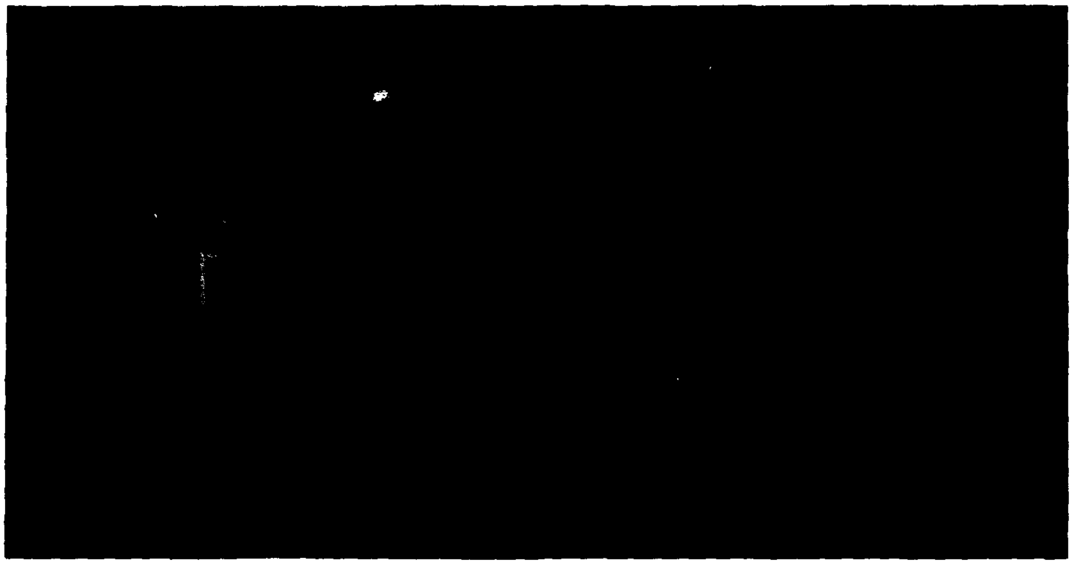

$V_I/V_O=0$

$V_I/V_O=8.1$

Fig.17(f) Effect of inlet flow at different angles of attack
Angle of attack = 30.5^{o} (Plan view)
(LEF/TEF = $35^{o}/0^{o}$; V_o = 80 mm/s; LEX fences off)

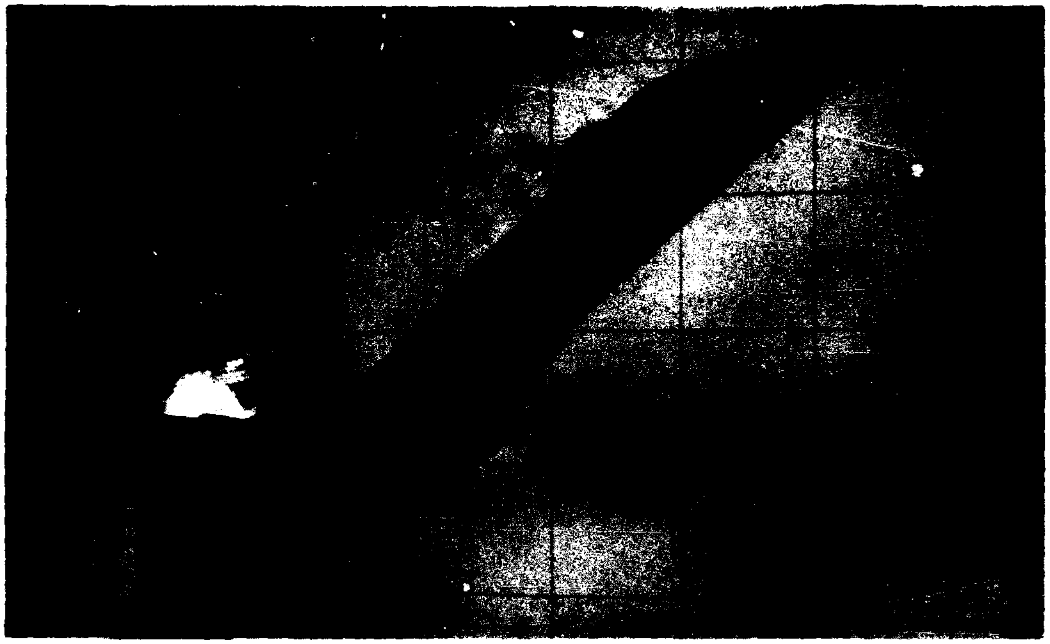

$V_I/V_O=0$

$V_I/V_O=8.1$

Fig.17(g) Effect of inlet flow at different angles of attack

Angle of attack =40.3^{O} (Side view)

(LEF/TEF = 35^{O}/0^{O}; V_o = 80 mm/s; LEX fences off)

$V_I/V_O=0$

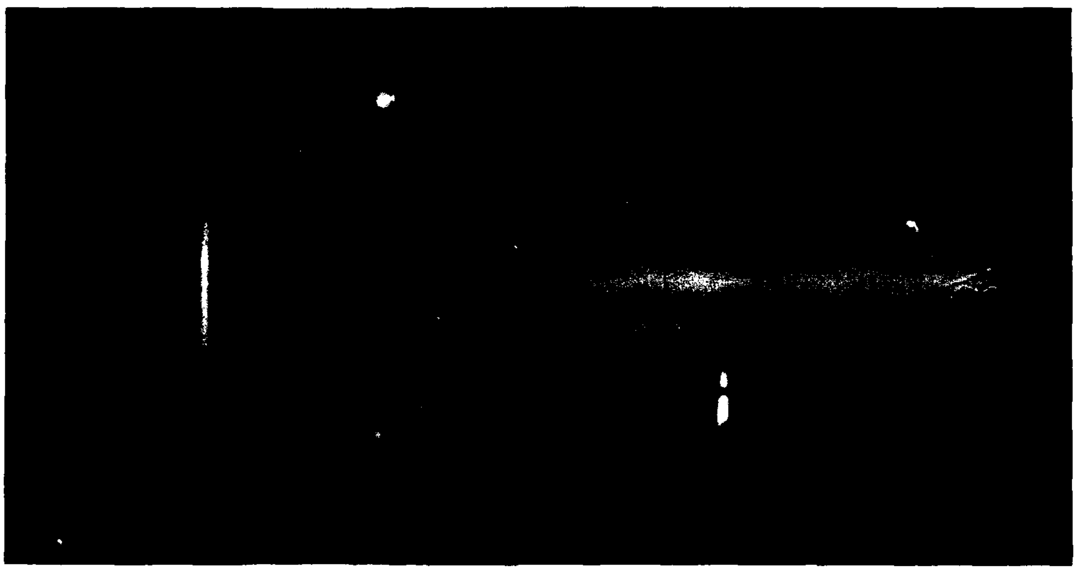

$V_I/V_O=8.1$

Fig.17(h) Effect of inlet flow at different angles of attack
Angle of attack $=40.3^{o}$ (Plan view)
(LEF/TEF = $35^{o}/0^{o}$; V_o = 80 mm/s; LEX fences off)

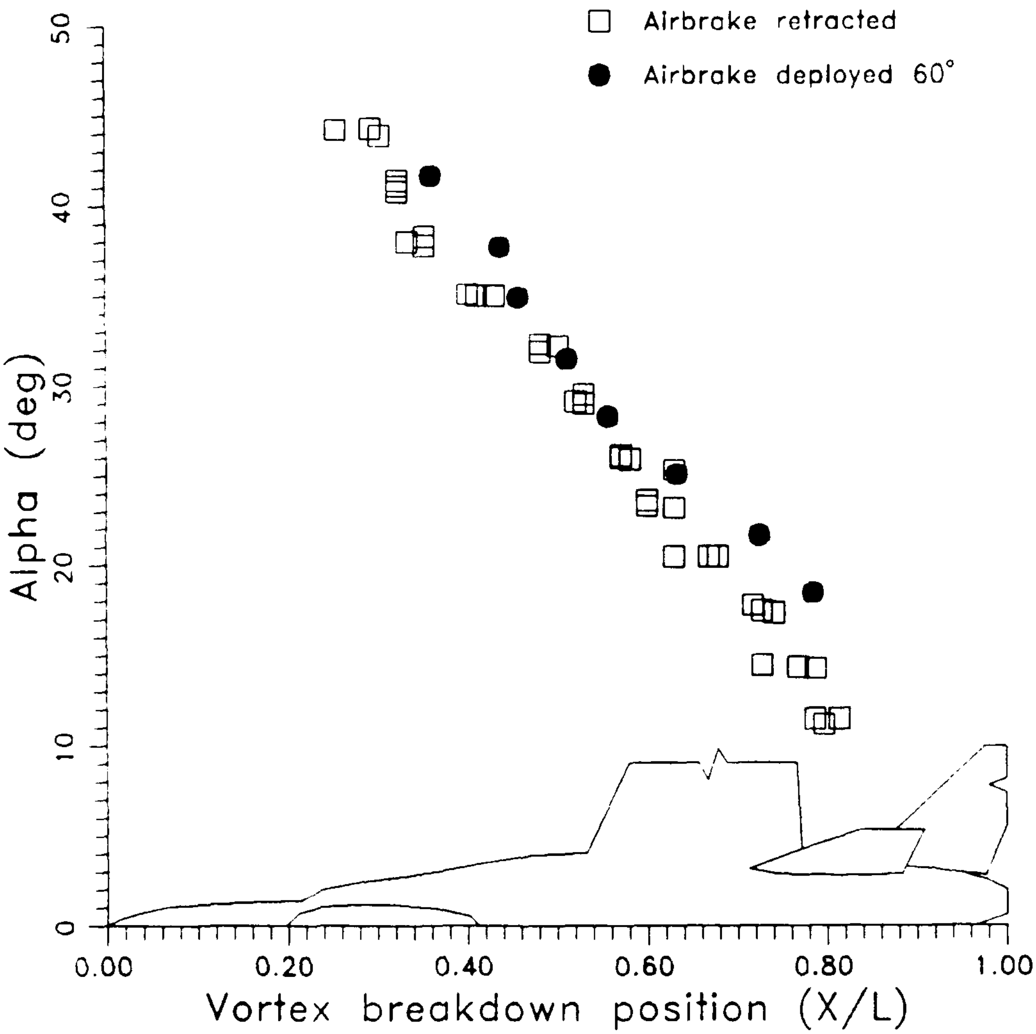

Fig 18 Vortex breakdown position over F/A-18

Effect of airbrake deflection

(LEF/TEF = $35^o/0^o$; V_o = 80 mm/s; LEX fences off; V_I/V_o = 0)

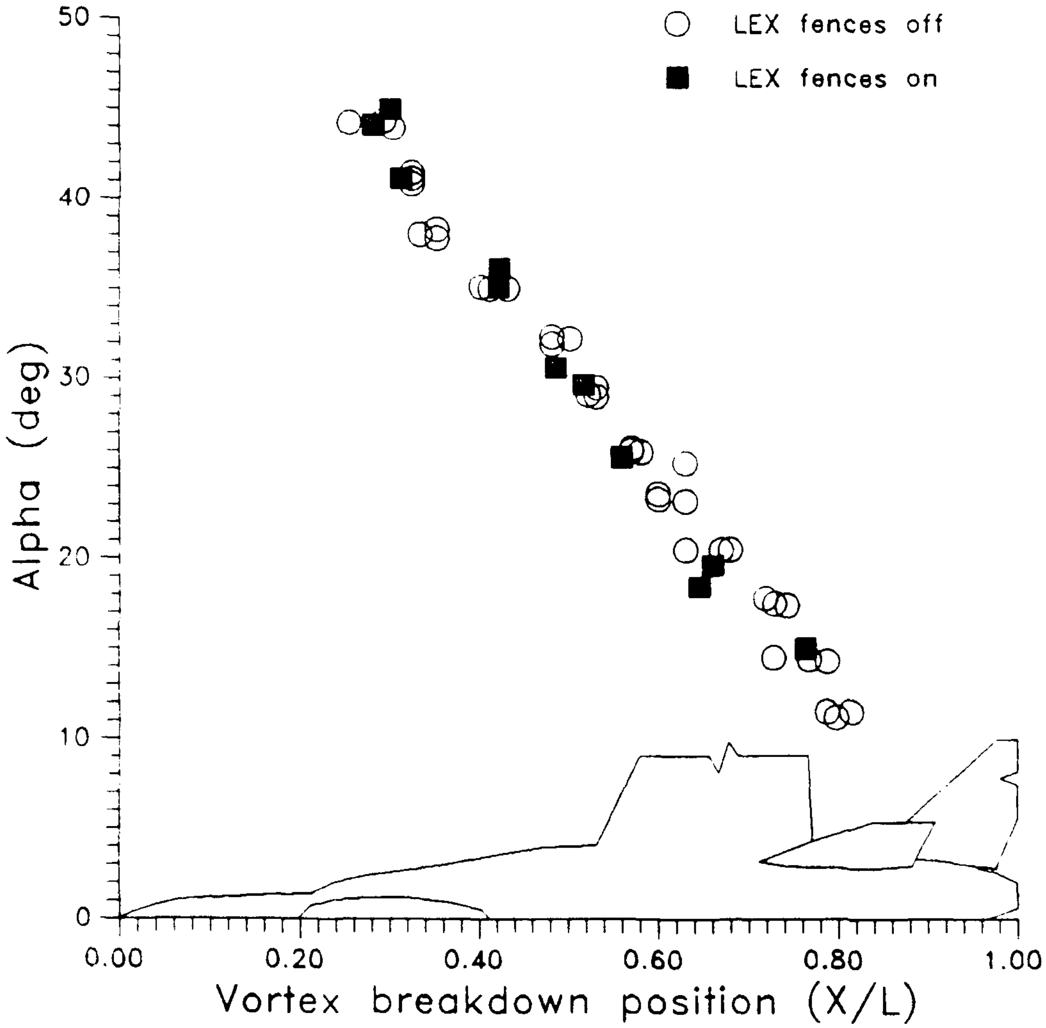

Fig.19 Vortex breakdown position over F/A-18
Effect of LEX fences
(LEF/TEF = $35^{o}/0^{o}$; V_{o} = 80 mm/s; V_{I}/V_{o} = 0)

LEX fence off

LEX fence on

Fig.20(a) Effect of LEX fence on vortex flows over F/A-18
Angle of attack = 19.5° (Side view)
(LEF/TEF = 35°/0°; V_o = 80 mm/s; V_I/V_o = 0)

LEX fence off

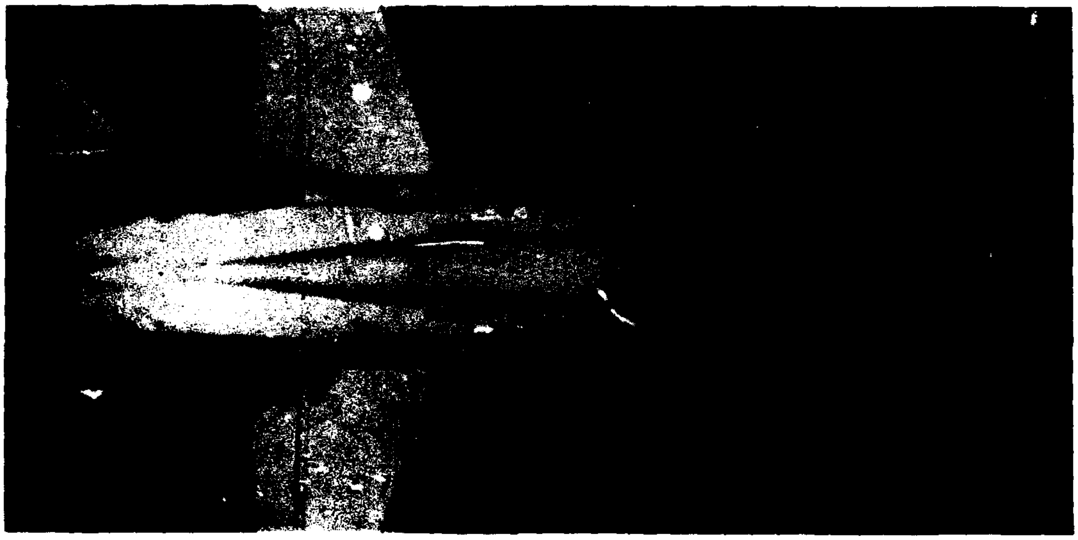

LEX fence on

Fig.20(b) Effect of LEX fence on vortex flows over F/A-18
Angle of attack = 19.5^{o} (Plan view)
(LEF/TEF = $35^{o}/0^{o}$; V_o = 80 mm/s; V_I/V_o = 0)

LEX fence off

LEX fence on

Fig.20(c) Effect of LEX fence on vortex flows over F/A-18
Angle of attack = 25.4^o (Side view)
(LEF/TEF = $35^o/0^o$; V_o = 80 mm/s; V_I/V_o = 0)

LEX fence off

LEX fence on

Fig.20(d) Effect of LEX fence on vortex flows over F/A-18
Angle of attack = 25.4^{o} (Plan view)
(LEF/TEF = $35^{o}/0^{o}$; V_{o} = 80 mm/s; V_{I}/V_{o} = 0)

LEX fence off

LEX fence on

Fig.20(e) Effect of LEX fence on vortex flows over F/A-18
Angle of attack = 30.5^{o} (Side view)
(LEF/TEF = $35^{o}/0^{o}$; V_o = 80 mm/s; V_I/V_o = 0)

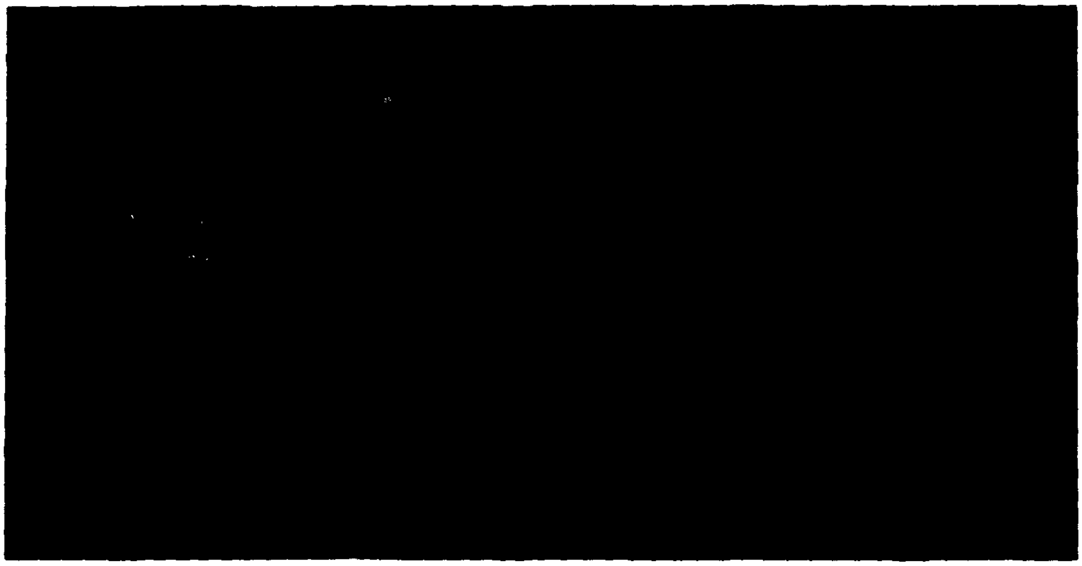

LEX fence off

LEX fence on

Fig.20(f) Effect of LEX fence on vortex flows over F/A-18
Angle of attack = 30.5^{o} (Plan view)
(LEF/TEF = $35^{o}/0^{o}$; V_o = 80 mm/s; V_I/V_o = 0)

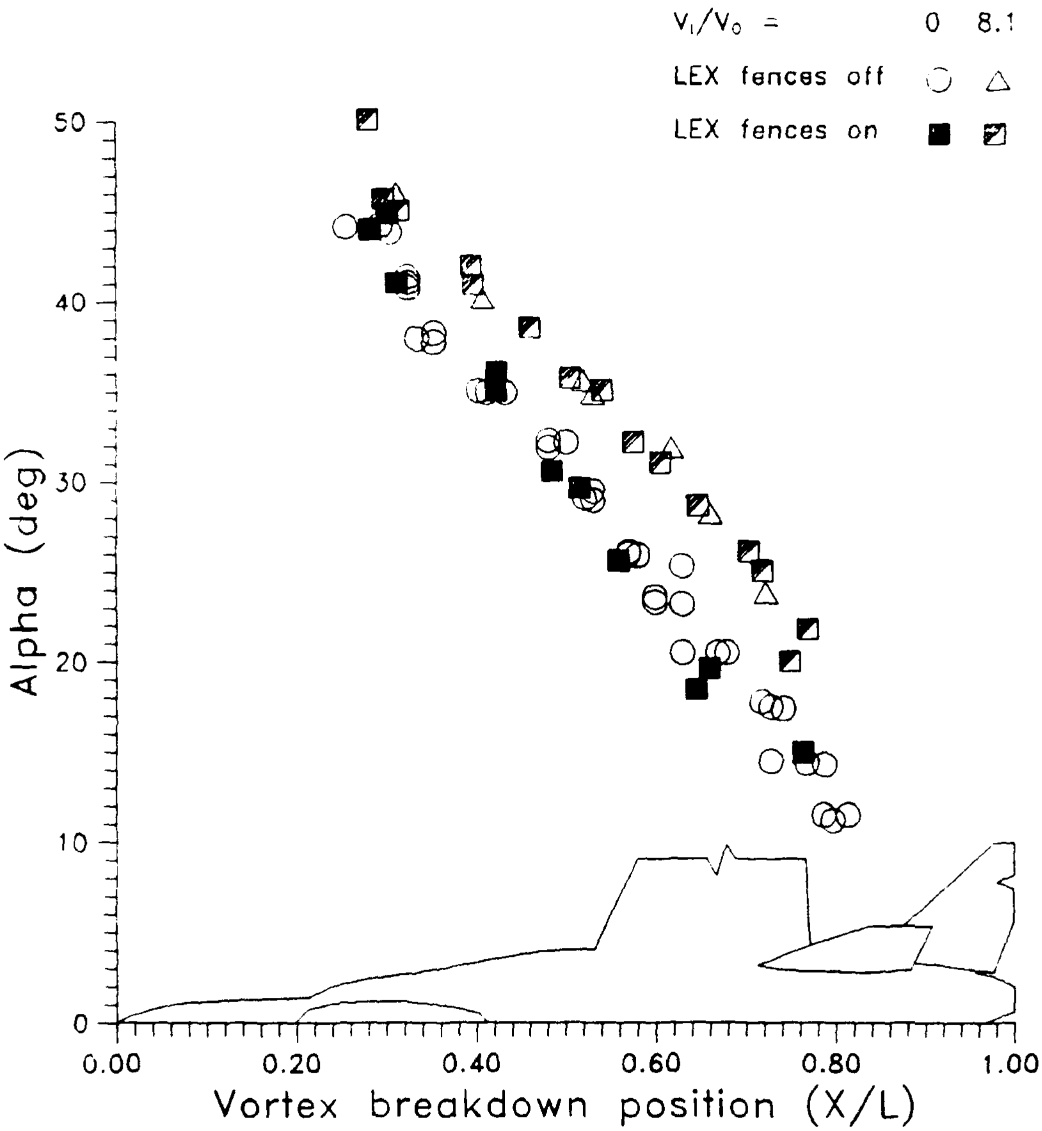

Fig.21 Vortex breakdown position over F/A-18
Effect of engine inlet flow (fences on)
(LEF/TEF = $35^o/0^o$; V_o = 80 mm/s)

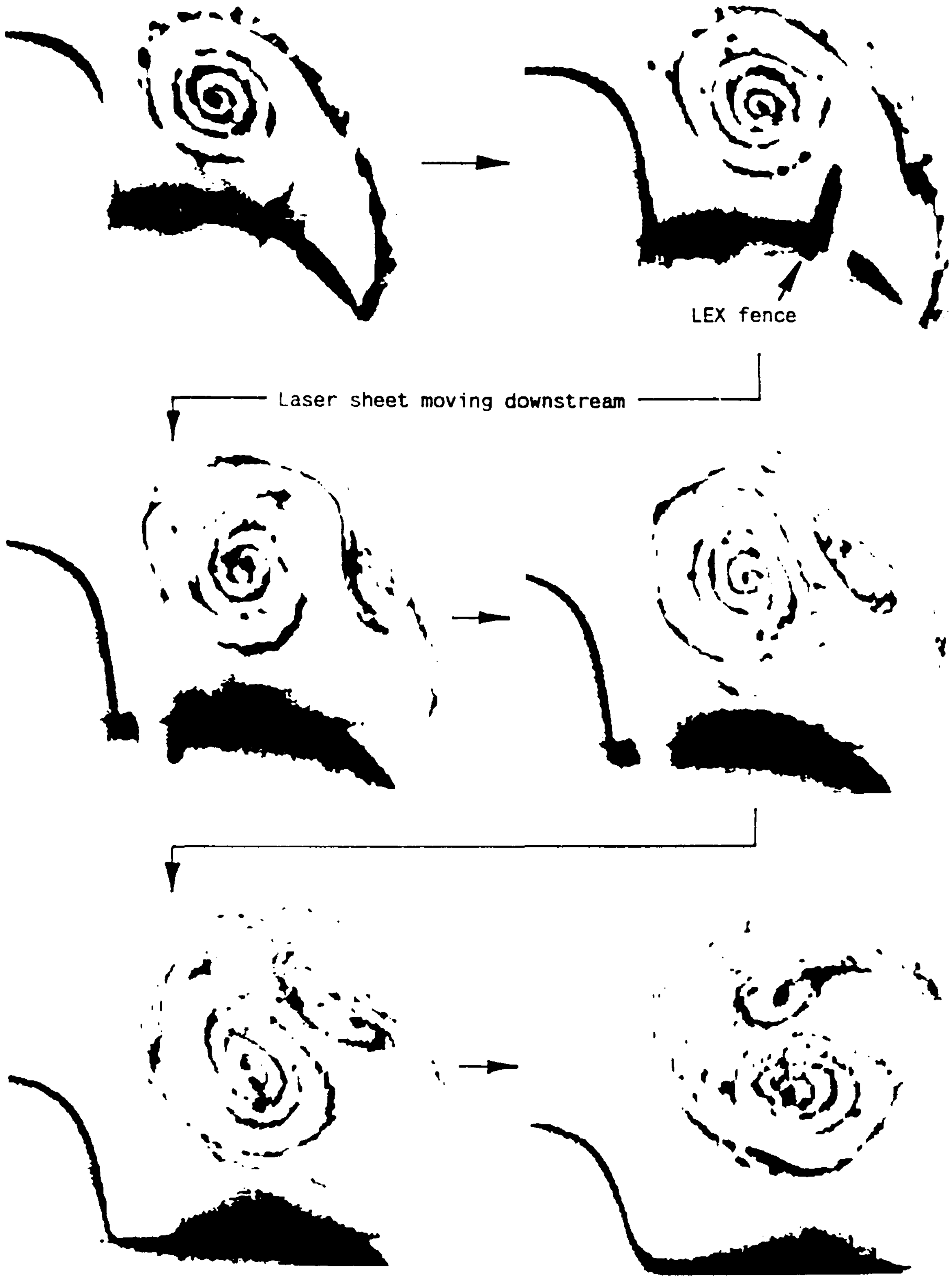

Fig.22 Cross-sections of LEX vortex system near fence

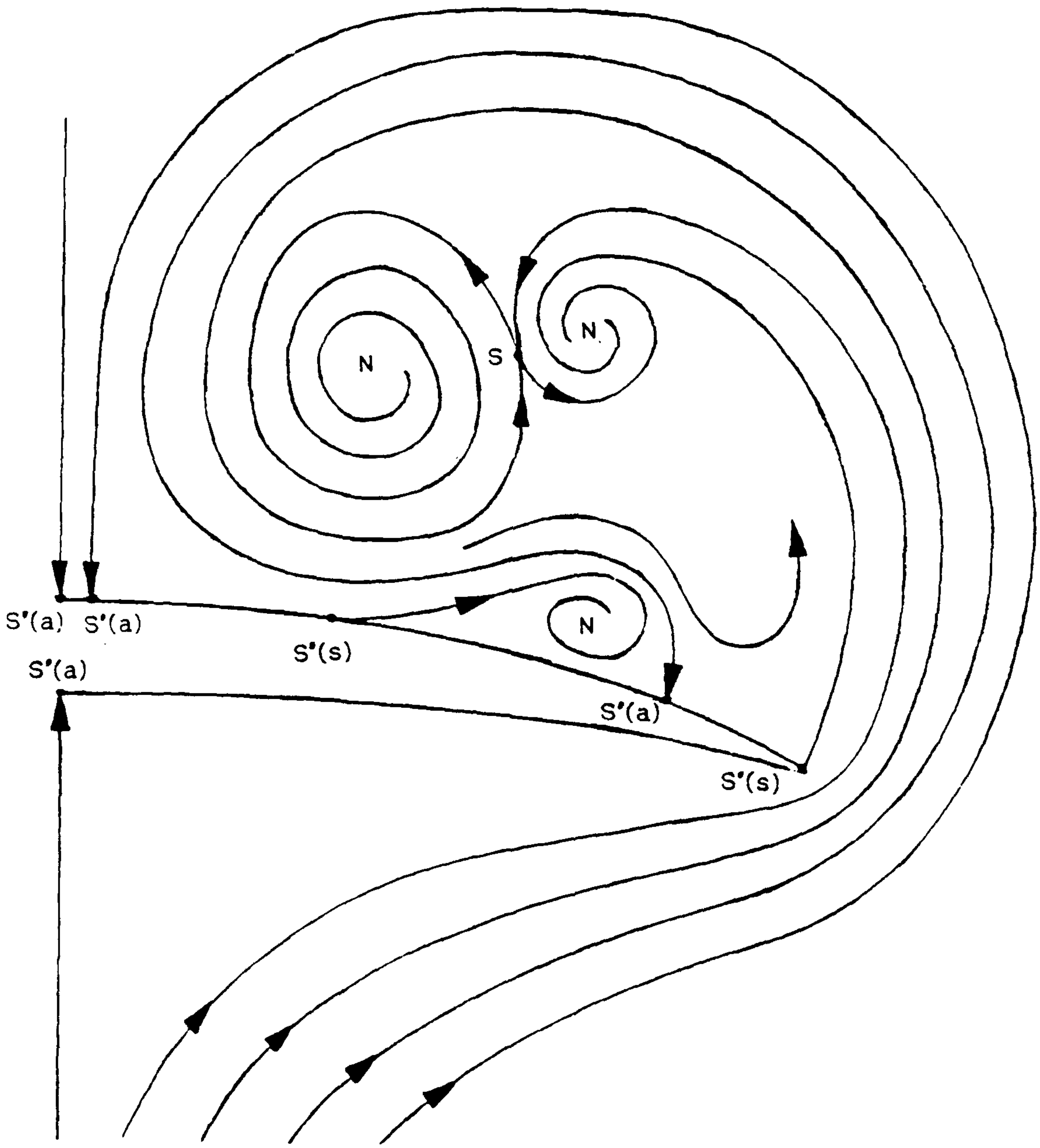

Fig.23 Possible topology of cross-flow downstream of fence

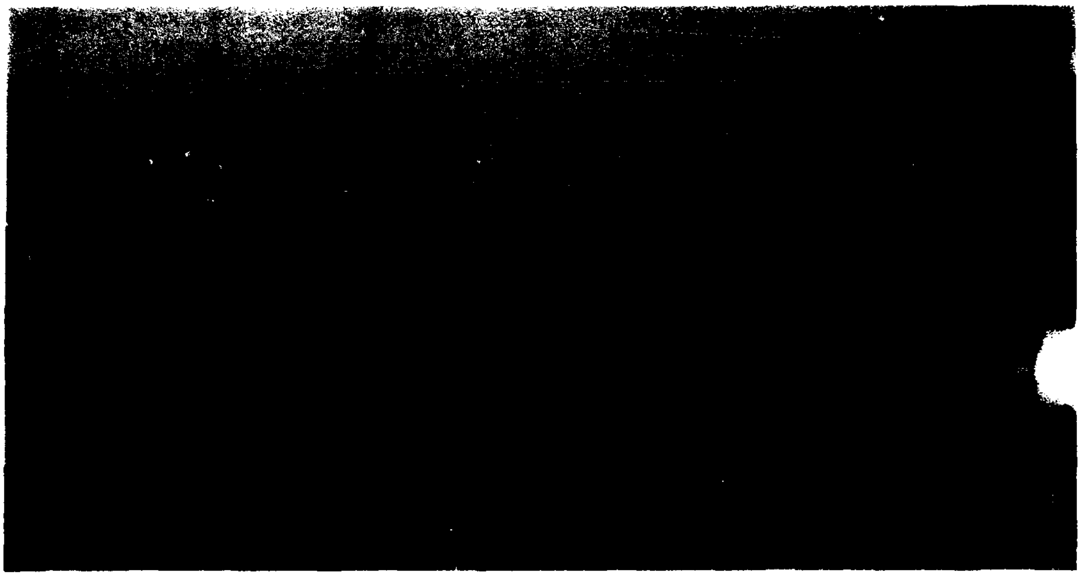

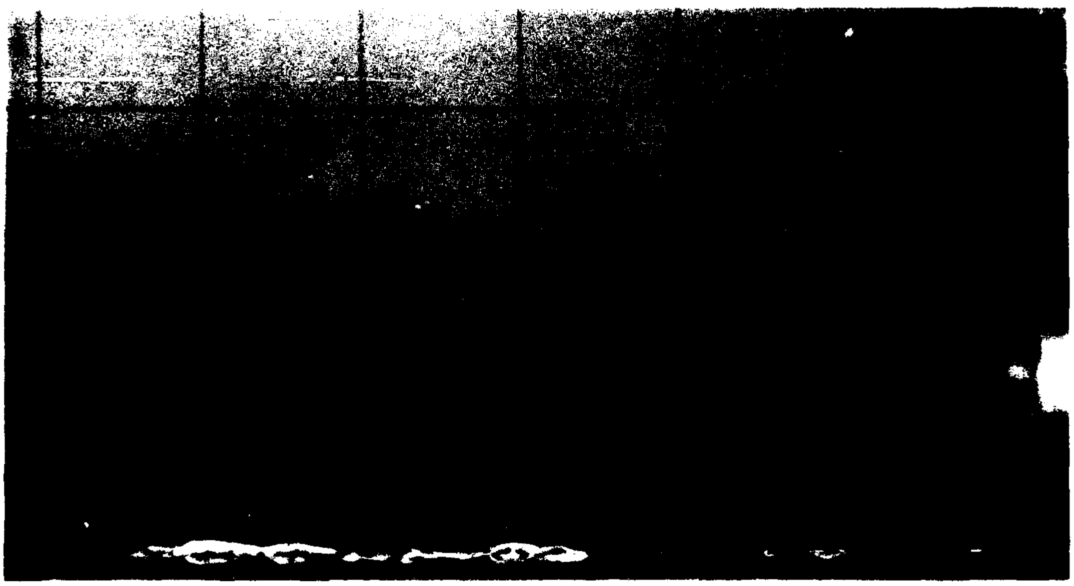

Fig.24 Breakdown in second vortex with fences on

Angle of attack = 19.5^o

(LEF/TEF = $35^o/0^o$; V_o = 30 mm/s; V_I/V_o = 0)

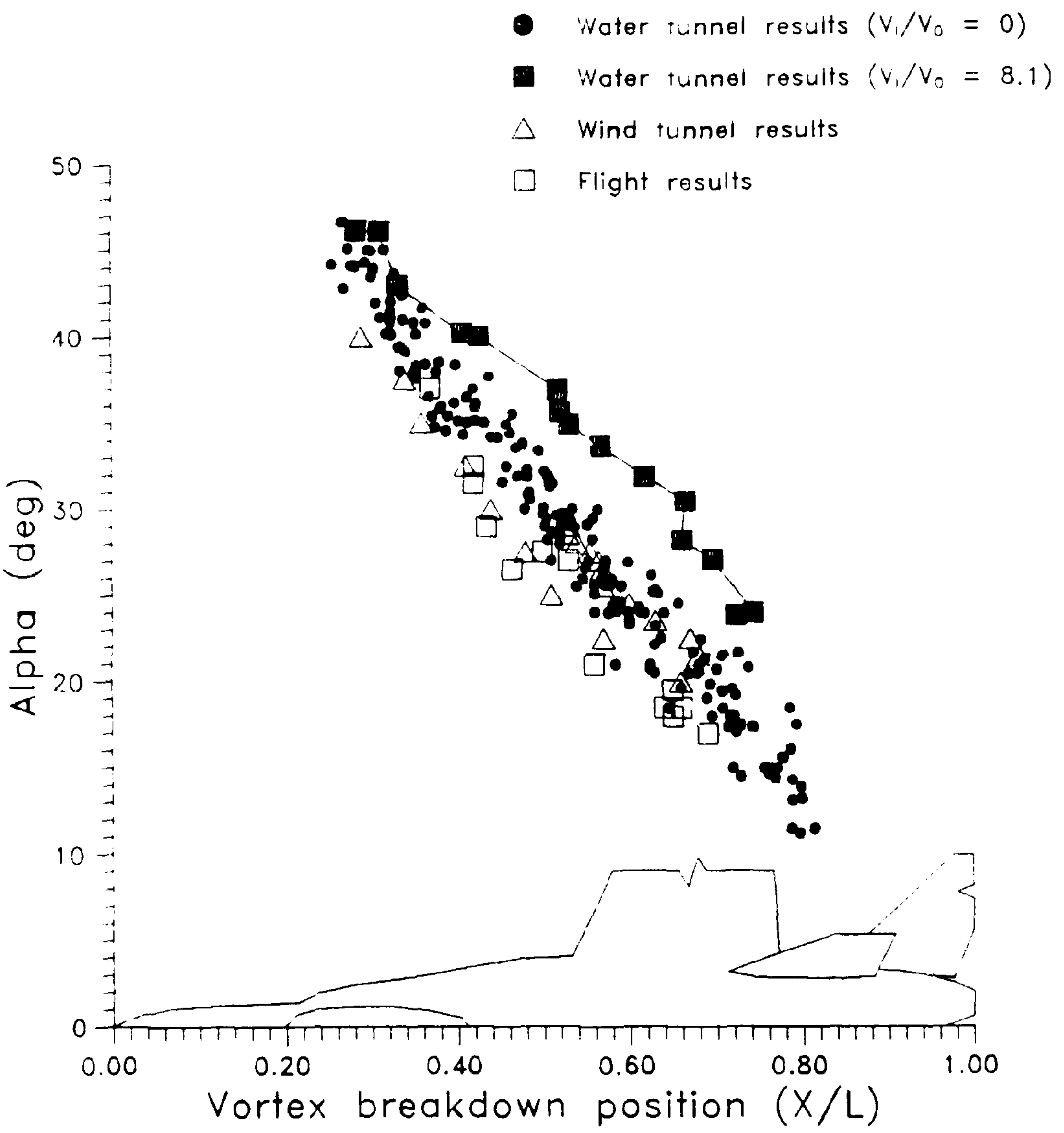

Fig.25 Vortex breakdown position over F/A-18
Results for all configurations and sources

DISTRIBUTION

AUSTRALIA

DEPARTMENT OF DEFENCE

Defence Central
- Chief Defence Scientist
- FAS, Science Policy (shared copy)
- AS, Science Corporate Management (shared copy)
- Director, Departmental Publications
- Counsellor, Defence Science, London (Doc Data Sheet Only)
- Counsellor, Defence Science, Washington (Doc Data Sheet Only)
- OIC TRS, Defence Central Library
- Document Exchange Centre, DTIC (8 copies)
- Defence Intelligence Organisation
- Librarian H Block, Victoria Barracks, Melbourne

Aeronautical Research Laboratory
- Director
- Library
- Chief, Flight Mechanics and Propulsion Division
- Head, Flight Mechanics Branch
- Branch File - Flight Mechanics Branch
- Author: D.H.Thompson (10 copies)
- B.D. Fairlie
- C.A. Martin (8 copies for distribution to TTCP HTP-5)
- J.M. Lopez
- M.K. Glaister
- L. MacLaren

Air Force Office
- Air Force Scientific Adviser (Doc Data Sheet Only)
- Aircraft Research and Development Unit
  - Scientific Flight Group
  - Library
- RAAF Academy, Pt. Cook

Industry

Aerospace Technologies Australia
- Library (2 copies)

Hawker de Havilland Australia Pty. Ltd., Victoria
- Library

Universities and Colleges

Melbourne
- Engineering Library

Monash
- Hargrave Library

Sydney
Engineering Library

NSW
Physical Sciences Library
Library, Australian Defence Force Academy

RMIT
Library
Mr M.L. Scott, Aerospace Engineering

Newcastle
Library (2 copies)

CANADA

NRC National Aeronautical Establishment
Library
Mr B.H.K. Lee

University of Toronto, Institute for Aerospace Studies
Library

FRANCE
ONERA
Library

INDIA
National Aeronautical Laboratory
Information Centre

JAPAN
National Aerospace Laboratory
Library

NETHERLANDS
National Aerospace Laboratory (NLR)
Library
Dr H.W.M. Hoeijmakers

Delft University of Technology
Mr N.G. Verhaagen, Dept. of Aerospace Engineering

SWEDEN
Aeronautical Research Institute
Library

SWITZERLAND
F & W (Swiss Aircraft Factory)

UNITED KINGDOM
CAARC, Secretary
Royal Aerospace Establishment
Bedford
Library
Farnborough
Library
Mr J.H.B. Smith
Aircraft Research Association
Library
British Aerospace (Warton)
Library

Universities and Colleges

Bristol
Engineering Library
Professor M.V. Lowson, Dept. of Aerospace Engineering

Cambridge
Engineering Library

Southampton
Library

Imperial College
Aeronautics Library

Cranfield Inst. of Technology
Library

UNITED STATES OF AMERICA
NASA Scientific and Technical Information Facility
NASA Ames Research Center
Mr L.B. Schiff
Fluid Mechanics Lab, Dr B.G. McLachlan
Mr L. Meyn
NASA Langley Research Center
Mr J.R. Chanbers
Mr W.L Sellers
Mr G.E. Erickson
Mr J.E. Lamar

Eidetics International
Mr G.N. Malcolm

Vigyan Research Associates Inc.
Dr D.M. Rao

McDonnell Aircraft Co.
Mr R.J. Paul (F/A-18 Aerodynamics Group)

Naval Air Systems Command Headquarters
Mr R.J. Hanley (F/A-18 Aerodynamics)

Universities and Colleges

University of Notre Dame
Professor R.C. Nelson, Dept. of Aerospace Engineering

Wichita State University
Professor W.H. Wentz, Institute for Aviation Research

SPARES (10 copies)

TOTAL (102 copies)

AL 149 DEPARTMENT OF DEFENCE

DOCUMENT CONTROL DATA

PAGE CLASSIFICATION	UNCLASSIFIED
PRIVACY MARKING	

1a. AR NUMBER	1b. ESTABLISHMENT NUMBER	2. DOCUMENT DATE	3. TASK NUMBER
AR-005-607	ARL-FLIGHT-MECH-R-179	DECEMBER 1990	DST 88/034

4. TITLE	5. SECURITY CLASSIFICATION (PLACE APPROPRIATE CLASSIFICATION IN BOX(S) IE. SECRET (S), CONF. (C) RESTRICTED (R), UNCLASSIFIED (U)).	6. NO. PAGES
WATER TUNNEL FLOW VISUALISATION OF VORTEX BREAKDOWN OVER THE F/A-18	U (DOCUMENT) U (TITLE) U (ABSTRACT)	61
		7. NO. REFS. 10

8. AUTHOR(S)
D.H. THOMPSON

9. DOWNGRADING/DELIMITING INSTRUCTIONS
Not applicable

10. CORPORATE AUTHOR AND ADDRESS
AERONAUTICAL RESEARCH LABORATORY
506 LORIMER STREET
FISHERMENS BEND VIC 3207

11. OFFICE/POSITION RESPONSIBLE FOR:
SPONSOR DSTO
SECURITY -
DOWNGRADING -
APPROVAL DARL

12. SECONDARY DISTRIBUTION (OF THIS DOCUMENT)
Approved for public release

OVERSEAS ENQUIRIES OUTSIDE STATED LIMITATIONS SHOULD BE REFERRED THROUGH DSTIC, ADMINISTRATIVE SERVICES BRANCH, DEPARTMENT OF DEFENCE, ANZAC PARK WEST OFFICES, ACT 2601

13a. THIS DOCUMENT MAY BE ANNOUNCED IN CATALOGUES AND AWARENESS SERVICES AVAILABLE TO ....
No limitations

13b. CITATION FOR OTHER PURPOSES (IE. CASUAL ANNOUNCEMENT) MAY BE [X] UNRESTRICTED OR [ ] AS FOR 13a.

14. DESCRIPTORS
Water tunnel tests
Flow visualization
Vortex breakdown
F/A-18 aircraft

15. DISCAT SUBJECT CATEGORIES
010303
010101

16. ABSTRACT
Vortex flow patterns over models of the F/A-18 aircraft were visualised using dye and hydrogen bubble techniques in a water tunnel. The axial position of vortex breakdown in the leading-edge extension (LEX) vortices was measured, and was found to be insensitive to Reynolds number, to flap setting, and to small variations in model cross-section shape. Engine inlet flow did alter the vortex breakdown position, at flow rates that might be encountered under flight conditions. The fitting of fences on the LEX upper surface did not affect the axial position of vortex breakdown, but did alter the vortex structure. These alterations were examined in some detail.

PAGE CLASSIFICATION
UNCLASSIFIED
PRIVACY MARKING

THIS PAGE IS TO BE USED TO RECORD INFORMATION WHICH IS REQUIRED BY THE ESTABLISHMENT FOR ITS OWN USE BUT WHICH WILL NOT BE ADDED TO THE DISTIS DATA UNLESS SPECIFICALLY REQUESTED.

16. ABSTRACT (CONT).

17. IMPRINT

AERONAUTICAL RESEARCH LABORATORY, MELBOURNE

18. DOCUMENT SERIES AND NUMBER	19. COST CODE	20. TYPE OF REPORT AND PERIOD COVERED
Flight Mechanics Report 179	54-5011	

21. COMPUTER PROGRAMS USED

22. ESTABLISHMENT FILE REF.(S)

23. ADDITIONAL INFORMATION (AS REQUIRED)